



## Sediment release of dissolved organic matter to the oxygen minimum zone off Peru

Alexandra N. Loginova<sup>1</sup>, Andrew W. Dale<sup>1</sup>, Frédéric A. C. Le Moigne<sup>1,2</sup>, Sören Thomsen<sup>1,3</sup>, Stefan Sommer<sup>1</sup>, Klauss Wallmann<sup>1</sup>, and Anja Engel<sup>1</sup>

<sup>1</sup>GEOMAR Helmholtz Centre for Ocean Research Kiel, Germany

<sup>2</sup>Mediterranean Institute of Oceanography, UM110, Aix Marseille Université, CNRS, IRD, 13288, Marseille, France

<sup>3</sup>LOCEAN-IPSL, IRD/CNRS/Sorbonnes Universités (UPMC)/MNHN, Paris, France

**Correspondence:** Anja Engel (aengel@geomar.de)

### Abstract.

The eastern tropical South Pacific (ETSP) represents one of the most productive areas in the ocean that is characterized by a pronounced oxygen minimum zone (OMZ). Particulate organic matter (POM) that sinks out of the euphotic zone is supplied to the anoxic sediments and utilized by microbial communities. The degradation of POM is associated with dissolved organic matter (DOM) production and reworking. The release of recalcitrant DOM to the overlying waters may represent an important organic matter escape mechanism from remineralization within sediments but received little attention in OMZ regions so far. Here, we combine measurements of dissolved organic carbon (DOC) and dissolved organic nitrogen (DON) with DOM optical properties in the form of chromophoric (CDOM) and fluorescent (FDOM) DOM from pore waters and near-bottom waters of the ETSP off Peru. We evaluate diffusion-driven fluxes and net *in situ* fluxes of DOC and DON in order to investigate processes affecting DOM cycling at the sediment–water interface along a transect 12°S. To our knowledge, these are the first data for sediment release of DON and pore water CDOM and FDOM for the ETSP off Peru. Pore-water DOC and DON accumulated with increasing sediment depth, suggesting an imbalance between DOM production and remineralization within sediments. High DON accumulation resulted in very low pore water DOC/DON ratios ( $\leq 1$ ) which could be caused by either an "imbalance" in DOC and DON remineralization, or to the presence of an additional nitrogen source. Diffusion driven fluxes of DOC and DON exhibited high spatial variability. They varied from  $0.2 \pm 0.1 \text{ mmol m}^{-2} \text{ d}^{-1}$  to  $2.5 \pm 1.3 \text{ mmol m}^{-2} \text{ d}^{-1}$  and from  $-0.04 \pm 0.02 \text{ mmol m}^{-2} \text{ d}^{-1}$  to  $3.3 \pm 1.7 \text{ mmol m}^{-2} \text{ d}^{-1}$ , respectively. Generally low net *in situ* DOC and DON fluxes as well as steepening of spectral slope ( $S$ ) of CDOM and accumulation of humic-like FDOM at the near-bottom waters over time indicated active microbial DOM utilization at the sediment–water interface, potentially stimulated by nitrate ( $\text{NO}_3^-$ ) and nitrite ( $\text{NO}_2^-$ ). The microbial DOC utilization rates, estimated in our study, may be sufficient to support denitrification rates of  $0.2\text{--}1.4 \text{ mmol m}^{-2} \text{ d}^{-1}$ , suggesting that sediment release of DOM contributes substantially to nitrogen loss processes in the ETSP off Peru.



## 1 Introduction

The eastern tropical South Pacific (ETSP) is one of the most productive areas of the world ocean (Pennington et al., 2006). High productivity, followed by intense organic matter remineralisation (e.g. Loginova et al., 2019; Maßmig et al., 2019a) in combination with sluggish ventilation (Stramma et al., 2005; Keeling et al., 2010) leads to a formation of pronounced oxygen  
5 minimum zone (OMZ) (e.g. Stramma et al., 2008). Remineralization of organic matter under anoxia induces nitrogen (N)-loss by denitrification and anammox as well as dissimilatory nitrate reduction to ammonium (DNRA) in the water column and sediments off the coast of Peru (Kalvelage et al., 2013; Arévalo-Martínez et al., 2015; Dale et al., 2016; Sommer et al., 2016; Glock et al., 2019). Although organic matter remineralization is classically assumed to be limited by the absence of oxygen (Demaison and Moore, 1980), recent studies report similar abilities of marine microbes to degrade organic matter in  
10 oxygenated surface waters and within OMZs (Pantoja et al., 2009; Maßmig et al., 2019a, b), suggesting that other factors, such as the quality of organic matter may regulate microbial activity within OMZs (Pantoja et al., 2009; Le Moigne et al., 2017). Extensive fieldwork campaigns conducted on anoxic Peruvian sediments suggested further show that they act as "factories" for an intensive organic matter remineralization (Dale et al., 2015). Yet, the burial efficiency of particulate organic carbon (POC) varies throughout OMZ (Dale et al., 2015). For instance, burial efficiency are low at anoxic inner shelf stations despite highest  
15 carbon mineralization rates estimated from *in situ* dissolved inorganic carbon (DIC) fluxes (Dale et al., 2015).

The degradation of particulate organic matter (POM) is associated with the production and reworking of dissolved organic matter (DOM) (Smith et al., 1992). Fluxes of dissolved organic carbon (DOC) out of the sediment generally account for around 10% of DIC fluxes (Komada et al., 2016), and, hence, represents an important escape mechanism for carbon from sediments (e.g. Ludwig et al., 1996; Burdige et al., 1999). The DOM release from Peruvian sediments has not been quantified so far and  
20 the cycling of DOM within the sediments off Peru has not been addressed in detail.

Generally, DOM in sediments is assumed to be recalcitrant (e.g. Burdige and Komada, 2015). However, elevated concentrations of dissolved organic nitrogen (DON) within sediments suggest the presence of bio-available proteinaceous organic matter in pore waters, that have escaped degradation within the water column (e.g. Faganeli and Herndl, 1991). The elemental ratio DOC/DON that is commonly used for inferring organic matter bio-availability in the water column, in sediment pore waters,  
25 displays controversial patterns. Thus, some studies suggest that oxygenated sediments show lower DOC/DON ratios compared to those of anoxic sediments (Burdige and Gardner, 1998). However, other studies found lower DOC/DON ratios (2-5) in sediments with reduced O<sub>2</sub>, compared to well oxygenated study sites (Faganeli and Herndl, 1991; Alkhatib et al., 2013).

The fraction of DOM that exhibits optical activity owing to the presence of chromophoric groups — a combination of conjugated double bonds and hetero-atoms — in its molecular structure is referred to as chromophoric DOM (CDOM) and  
30 fluorescent DOM (FDOM). These optical properties were shown to provide important information on DOM cycling and transformations in the water column (e.g. Coble, 1996; Zsolnay et al., 1999; Jørgensen et al., 2011; Catalá et al., 2016; Loginova et al., 2016) and sediments (e.g. Chen et al., 2016). CDOM refers to DOM that absorbs light over a broad spectra from UV to visible wavelengths. CDOM absorbance spectra represent an exponential curve with no discernible peaks (Del Vecchio and Blough, 2004) and the shape of the spectra (*S*) and absorption coefficients are used to learn on bulk DOM properties. For in-



stance, steepness of the  $S$  is suggestive of relative differences in DOM molecular weight. Thus, a decrease of CDOM absorption in the visible spectra, compared to UV wavelength implies a decrease in DOM molecular weight (e.g. Helms et al., 2008). This is due to the ability of high molecular weight (HMW)DOM to absorb light at longer wavelengths, compared to low molecular weight (LMW)DOM. The part of CDOM that may fluoresce due to its aromatic nature is referred to as FDOM and is used to infer DOM quality (Coble, 1996; Zsolnay et al., 1999; Jørgensen et al., 2011; Catalá et al., 2016; Loginova et al., 2016). Thus, 3D fluorescence spectroscopy, followed by parallel factor analysis (PARAFAC), has been recognized as a useful tool for distinguishing between different organic matter pools (Murphy et al., 2013). Fluorophores that are excited and emit at UV wavelengths are often referred to as amino acid-like DOM. Components that are excited at UV, but emit at visible wavelengths, are mainly referred to as humic-like or fulvic-like DOM (e.g. Coble, 1996; Murphy et al., 2014, and references therein).

The distribution of CDOM within pore-waters provides important insights on processes related to organic matter remineralization. For instance, anoxic sediments in the Chukchi Sea were previously found to be a production site of humic-like substances and a potential source of pre-altered DOM into the water column (Chen et al., 2016). On the other hand, FDOM measurements made during incubation of sediment cores from Uiam Lake (Yang et al., 2014), suggested that DOM released into the overlying water may be further altered by microbial communities, and, therefore, serves as an important source of bioavailable organic matter. In the ETSP off Peru, fine spatial resolution FDOM measurements also suggested high DOM release from anoxic sediments into the water column (Loginova et al., 2016). High FDOM fluorescence associated with benthic release of DOM reached the euphotic zone, likely influencing organic carbon turnover of the whole water column. Hence, sediment release of DOM could potentially serve an important carbon and N source (e.g. Moran and Zepp, 1997) and an insolation shield (e.g. Belzile et al., 2002) for pelagic microbial communities, affecting biogeochemical processes of the water column.

The release of dissolved substances from anoxic sediments is regulated mainly by diffusion through the sediment–water interface (e.g. Lavery et al., 2001, and references therein). Diffusion–driven solute fluxes (hereon "diffusive fluxes") are commonly evaluated from pore-waters gradient using Fick's First Law. Diffusive DOM fluxes have been found to be consistent with total DOM flux in non-bioturbated anoxic sediments (Burdige et al., 1992), such as those found off Peru (Dale et al., 2015; Sommer et al., 2016). In some sediments, however, the diffusive flux may overestimate the total flux (Burdige et al., 1992; Lavery et al., 2001). This may be attributed to bioturbation, "unfavourable" redox conditions (Lavery et al., 2001), irreversible adsorption onto particles, and biological DOM consumption at the sediment–water interface or in the bottom waters (Burdige et al., 1992). Furthermore, the assumptions or calculations of certain DOM parameters, such as molecular weight (Balch and Guéguen, 2015) and tortuosity (Ullman and Aller, 1982) may induce potential bias to the flux calculations. *In situ* measurements of the net solute flux using benthic incubation chambers are independent from molecular weight and tortuosity uncertainties. This approach is laborious and based on the assumption that solutes, released into the benthic chamber, behave conservatively during the time incubation, and, show linear trends over time. Herewith, the *in situ* measurements may be affected by an accidental enclosure of benthic macro-organisms, such as for instance *Pleuroncodes mondon*, which are abundant in the Peruvian OMZ (Kiko et al., 2015).



In this study, we determine diffusive and *in situ* fluxes of DOC and DON and combine those fluxes with DOM optical properties for the sediments in ETSP off Peru for the first time. Our objective is to provide a deeper understanding of DOM cycling in Peruvian sediments as well as potential transformations affecting DOM released into the water column.

## 2 METHODS

### 5 2.1 Study area

Sediment sampling was carried out in April–May 2017 during research cruises M136 and M137 to the Peruvian OMZ on board of RV Meteor. The sampling area was located between 12–12.2 °S and 77.1–77.3 °W (Fig. 1). In total, six stations (see Table 1) were sampled along the transect 12°S (12°S) on the inner shelf, outer shelf and continental slope (Dale et al., 2015, 2016; Sommer et al., 2016).

10 During the study, the water column at the sampling stations was subjected to a consistent poleward flow ranging from 0.1 to 0.5 m s<sup>-1</sup> (Lüdke et al., 2019). Low-oxygen ( $\ll 5 \mu\text{mol kg}^{-1}$ ) waters were observed above the sediment, with the exception for station 2 (St.2), where the O<sub>2</sub> concentration was slightly above 10  $\mu\text{mol kg}^{-1}$ . This may have been a remnant of the coastal el Niño that occurred 3–4 months prior to our fieldwork (Rodríguez-Morata et al., 2019) or an intensification of poleward flow, observed in May 2017 (Lüdke et al., 2019). The highest concentrations of nitrate (NO<sub>3</sub><sup>-</sup>) and nitrite (NO<sub>2</sub><sup>-</sup>) were observed at  
15 stations  $\geq 100$  m, while at shallower stations ammonium (NH<sub>4</sub><sup>+</sup>) concentrations up to 1.2–1.4  $\mu\text{mol L}^{-1}$  were observed (Lüdke et al., 2019). A detailed description of the sediment at 12°S is reported in Dale et al. (2015, 2016). In brief, sediments at the sampling stations are fine-grained muds with porosity ranging between 0.8 and >0.9 (Dale et al., 2015; Sommer et al., 2016) (also see Table 1). At some stations, the sediments were almost completely covered with sulphide-oxidizing *Thioploca* and *Beggiatoa* (Levin et al., 2002; Dale et al., 2015; Sommer et al., 2016).

### 20 2.2 Field sampling and sample preparation

Two benthic landers (Biogeochemical Observatory (BIGO) I and II) (Sommer et al., 2008) were deployed (see Table 1). Both were equipped with 2 circular flux chambers with an internal diameter of 28.8 cm. Volumes of the bottom water enclosed in the benthic chambers varied from  $\sim 12$  to  $\sim 20$  L during the study. Each BIGO chamber was equipped with eight glass syringes, which were filled sequentially to determine the net *in situ* flux of solutes across the sediment–water interface (Fig. 2). A detailed  
25 description of the BIGO lander can be found in Sommer et al. (2008) and Dale et al. (2014).

At each station, data from one BIGO chamber (chamber 2) were used for the DOM sampling. Samples for DOC, DON and CDOM and FDOM analyses were taken at  $\sim 0.2, 4, 9, 12, 17, 21, 25$  and 30 hrs after the beginning of sediment incubation.

Samples were passed through cellulose acetate membrane syringe filters (0.2  $\mu\text{m}$ ) into pre-combusted (450°C, 8 hrs) amber glass vials for CDOM and FDOM and into pre-combusted (450°C, 8 hrs) clear glass ampoules for DOC and DON analyses.  
30 The latter samples were fixed with 20  $\mu\text{l}$  of ultra-pure HCl (30 %: Merck Chemicals GmbH) and flame sealed before storage. All samples were stored (1–2 month) at +4°C in the dark pending analysis in the home laboratory.



The pore water DOM distribution and properties, as well as diffusive fluxes, were quantified by analysing DOC, DON, CDOM and FDOM in sediment cores obtained using multiple corers (MUCs). Retrieved sediments were immediately transferred to the onboard cool room (10-15 C°) and processed within few hours.

One sediment core from each station was sectioned into 12 slices over intervals ranging from 1 to 3 cm (Fig. 2). Sediments were transferred into acid-cleaned (10 % HCl) dry polypropylene (50 ml) centrifugation tubes and spun in a refrigerated centrifuge for 20 min at 4500 rpm. The supernatant was then passed through cellulose acetate membrane syringe filters (0.2 µm) into pre-combusted (450°C 8 hrs) clear glass ampoules for DOC and DON and amber glass vials for CDOM and FDOM. The samples were conserved and stored as described above.

### 2.3 Discrete sample analyses

CDOM absorbance was measured with a Shimadzu® 1700 UV-VIS double-beam spectrophotometer using a 1-cm Quartz SUPRASIL® precision cell (Hellma® Analytcs). Absorbance spectra were recorded at 1 nm wavelength intervals from 230 to 750 nm against MilliQ water as a reference. CDOM absorbance spectra from 275 to 400 nm were corrected for particle scattering (e.g. Nelson and Siegel, 2013) and recalculated to absorption according to Bricaud et al. (1981). We used the absorption coefficient at 325 nm ( $a_{\text{CDOM}(325)}$ ) to express CDOM "concentrations", as mainly used for open ocean areas (Nelson and Siegel, 2013). The spectral slope ( $S$ ) for the interval 275-295 nm ( $S_{275-295}$ ) was used to infer relative changes in DOM bulk quality, i.e. DOM relative molecular weight (Helms et al., 2008).  $S_{275-295}$ s were calculated following Helms et al. (2008) using log-transformed linear regression.

FDOM was analysed by Excitation-Emission Matrix (EEM) spectroscopy on a Cary Eclipse Fluorescence Spectrophotometer (Agilent Technologies) equipped with a xenon flash lamp. The fluorescence spectra for samples were measured in a 4-optical window 1-cm Quartz SUPRASIL® precision cell (Hellma®Analytcs). Blank fluorescence spectra and Water Raman scans were performed daily using an Ultra-Pure Water Standard sealed cell (3/Q/10/WATER; Starna Scientific Ltd). The experimental wavelength range for sample and ultra-pure water scans was 230 to 455 nm in 5 nm intervals on excitation and 290 to 700 nm in 2 nm intervals on emission. Water Raman scans were recorded from 285 to 450 nm at 1 nm intervals for emission at the 275 nm excitation wavelength (Murphy et al., 2013). All fluorescence measurements were conducted at 20 °C, controlled by a Cary Single Cell Peltier Accessory (VARIAN), PMT 900 V, with 0.2 s integration times and a 5 nm slit width on excitation and emission monochromators. The fluorescence spectra were corrected for spectral bias, background signals and inner filter effects and normalized to the area of the ultra-pure water Raman peaks. All samples were calibrated against a Quinine Sulphate Mono-hydrate dilution series, performed once during sample analyses. EEMs were analyzed by PARAFAC (Stedmon and Bro, 2008) and validated by split-half analysis using "drEEM toolbox for MATLAB" after Murphy et al. (2013). Four FDOM components that were identified during the PARAFAC analyses are expressed in Quinine Sulfate Equivalents (QSE).

Samples for inorganic N compounds in the benthic lander samples ( $\text{NO}_3^-$ ,  $\text{NO}_2^-$  and  $\text{NH}_4^+$ ) and in pore waters ( $\text{NH}_4^+$ ) were analysed following standard techniques after Hansen and Koroleff (2007) and will be published elsewhere (Clemens et al., in prep.).  $\text{NO}_3^-$  and  $\text{NO}_2^-$  concentrations in the pore waters were assumed to be negligible and not analysed (Dale et al., 2016).



DOC samples were analysed by the high-temperature catalytic oxidation (TOC -VCSH, Shimadzu) as described in detail by Engel and Galgani (2016). A TNM-1 N detector of Shimadzu analyser was used to determine total dissolved nitrogen (TDN) in parallel to DOC with a detection limit of  $2 \mu\text{mol L}^{-1}$  (Dickson et al., 2007). Concentrations of DON were calculated as a difference of TDN and the sum of concentrations of inorganic N components.

## 5 2.4 Evaluation of DOC and DON fluxes

In this study, diffusive and an *in situ* net DOC and DON fluxes were quantified. The diffusive fluxes of DOC ( $J_{DOC}(Diff.)$ ) and DON ( $J_{DON}(Diff.)$ ) from the uppermost slice of the sediment core (0 to 1 cm depth) to the bottom water were estimated by applying Fick's First Law:

$$J_s(Diff.) = -\phi \times D_s \times \frac{dC}{dz} \quad (1)$$

10 where  $J_s(Diff.)$  is a diffusive flux of a solute,  $\phi$  is the sediment porosity,  $\frac{dC}{dz}$  is the gradient of DOC (DON) concentration over the investigated depth interval (0 to 1 cm), and  $D_s$  is a bulk sediment diffusion coefficient.  $D_s$  was previously demonstrated to be dependent on the sediment formation resistivity factor ( $F$ ) (Ullman and Aller, 1982), as well on the average molecular weight of DOM (Burdige et al., 1992; Balch and Guéguen, 2015). In this study, we calculate  $D_s$  using  $F$  that equals  $\phi^{-3}$  (Ullman and Aller, 1982), as  $\phi$  measured at 12°S exceeded 0.8-0.9 (Table 1).

15 The molecular size fractionation was not addressed during this study, therefore, we assumed that DOM molecular weight varied in the range from 0.5 to 10 kDa. This assumption resulted in  $D_0$  varying from  $0.63 \times 10^{-6}$  to  $7.2 \times 10^{-6} \text{ cm}^{-2} \text{ s}^{-1}$  (Balch and Guéguen, 2015). This variance represented one of the major drivers of the estimated diffusive DOC (DON) flux variability and was accounted for standard deviation during calculations.

Net *in situ* fluxes of DOC ( $J_{DOC}(Net)$ ) and DON ( $J_{DON}(Net)$ ), measured in BIGO chambers, were evaluated as:

$$20 J_s(Net) = \frac{V}{A} \times \frac{dC}{dt} \quad (2)$$

where  $J_s(Net)$  net *in situ* flux of a solute,  $V$  is the chamber volume (in  $\text{m}^3$ ),  $A$  is the chamber area (in  $\text{m}^2$ ), and  $\frac{dC}{dt}$  is the DOC concentration gradient over time of the sediment enclosure (in  $\text{mmol m}^{-3} \text{ d}^{-1}$ ). The gradient was obtained by linear regression analyses ('polyfit' 1st order, MatLab, the MathWorks Inc.) of the DOC (DON) concentrations over time. The error of the linear regression was used as a representation of the standard deviation of the evaluated net fluxes.

25 In this study, fluxes directed out and into the sediment are reported as positive and negative values, respectively.

## 3 RESULTS

### 3.1 DOC and DON distribution and fluxes

Pore-water DOC and DON generally accumulated with depth in the sediment (Fig.3). Highest concentrations of DOC of  $967 \pm 682 \mu\text{mol L}^{-1}$  were measured at the inner shelf station 1 (St.1). DOC decreased gradually towards station 4 (St.4) where



concentrations were lowest ( $340 \pm 122 \mu\text{mol L}^{-1}$ ). Further offshore, DOC concentrations increased at station 5 (St.5) and station 6 (St.6), showing  $478 \pm 256$  and  $398 \pm 188 \mu\text{mol L}^{-1}$ , respectively.

Highest concentrations of DON were also measured at the inner shelf St.1 and St.2. The average DON concentrations in pore waters at these stations were  $708 \pm 685 \mu\text{mol L}^{-1}$  and  $813 \pm 291 \mu\text{mol L}^{-1}$ , respectively. Similarly to DOC, the concentrations decreased towards St.4 ( $10 \pm 24 \mu\text{mol L}^{-1}$ ), and then resumed the gradient offshore at St.5 ( $349 \pm 140 \mu\text{mol L}^{-1}$ ) and St.6 ( $62 \pm 92 \mu\text{mol L}^{-1}$ ).

The sediment pore waters at 12°S exhibited generally low DOC/DON ratios. The median DOC/DON ratios for most of the stations fell below 5. Generally, the median elemental ratio increased towards offshore from the minimum at St.2 (DOC/DON of  $<1$ ) to maximum at St.4 (median DOC/DON  $\sim 12$ ) and then decreased again at St.5 (median DOC/DON  $\sim 1$ ) and St.6 (median DOC/DON  $\sim 3$ ) (Fig.A1).

Near-bottom waters in the benthic incubation chambers did not display apparent differences in DOC concentrations between stations (Fig. 4). Average concentrations were  $92 \pm 22 \mu\text{mol L}^{-1}$ . Furthermore, DOC did not accumulate linearly over time at some stations (Fig.4). Similarly, DON concentrations varied from below detection to  $\sim 15 \mu\text{mol L}^{-1}$  in the chambers (Fig.4), resulting in much higher DOC/DON ratios than measured in pore waters. Median DOC/DON ratios in all chambers were  $\geq 5$  and gradually decreasing from a maximum at St.1 (median DOC/DON  $\sim 30$ ) towards offshore (Fig.A1).

The diffusive DOC fluxes varied from a minimum of  $0.2 \pm 0.1 \text{ mmol m}^{-2} \text{ d}^{-1}$  at St.2 to a maximum of  $2.5 \pm 1.3 \text{ mmol m}^{-2} \text{ d}^{-1}$  at station 3 (St.3) (Fig. 5). Net *in situ* DOC fluxes determined with benthic chambers were generally lower than diffusive fluxes and varied from  $-0.3 \pm 0.9$  at St.4 to  $2.3 \pm 2.3 \text{ mmol m}^{-2} \text{ d}^{-1}$  at St.2. However, no statistical differences were found between the different flux estimates at each station ( $p > 0.05$ , Mann-Whitney Rank Sum Test, SigmaPlot, Systat Software). Diffusive DON fluxes ranged from  $-0.04 \pm 0.02 \text{ mmol m}^{-2} \text{ d}^{-1}$  at St.1 and St.6 to  $3.3 \pm 1.7 \text{ mmol m}^{-2} \text{ d}^{-1}$  at St.2. Similar to DOC, net *in situ* DON fluxes were lower than diffusive DON fluxes and ranged from  $-0.05 \pm 0.3 \text{ mmol m}^{-2} \text{ d}^{-1}$  at St.6 to  $0.3 \pm 0.3 \text{ mmol m}^{-2} \text{ d}^{-1}$  at St.5.

### 3.2 Optical properties of DOM

To address DOM quality CDOM and FDOM fluorescence intensities were analysed in sediment pore waters and in the BIGO chambers.

In pore-waters, CDOM absorption ( $a_{\text{CDOM}(325)}$ ) exhibited a similar pattern to DOC distribution (Fig.3). Highest  $a_{\text{CDOM}(325)}$  ( $14 \pm 8 \text{ m}^{-1}$ ) was measured at St.1 and the lowest  $a_{\text{CDOM}(325)}$  values ( $5 \pm 2 \text{ m}^{-1}$ ) were measured at St.4. Further offshore, at St.5 and St.6  $a_{\text{CDOM}(325)}$  was higher than at St.4, resuming the offshore gradient.

In the benthic chambers,  $a_{\text{CDOM}(325)}$  was  $0.9 \pm 0.6 \text{ m}^{-1}$  on average (Fig.4). An apparent decrease of  $a_{\text{CDOM}(325)}$  over time occurred at St.1, St.3, St.5 and St.6, while at St.4 and St.2  $a_{\text{CDOM}(325)}$  exhibited an apparent increase and very low variance over time, respectively (Fig.4, Table A1).

CDOM spectral slope,  $S_{275-295}$ , in the pore waters displayed highest values ( $-0.016 \pm 0.004 \text{ nm}^{-1}$ ) at St.4, and the lowest values at St.1  $S_{275-295}$  ( $-0.018 \pm 0.001 \text{ nm}^{-1}$ ). These were comparable to the initial values of  $S_{275-295}$  in the BIGO benthic chambers ( $-0.018 \pm 0.005 \text{ nm}^{-1}$ ) (see Fig.3 and Fig.4).



The highest  $S_{275-295}$  was observed at the beginning of the sediment enclosure, and an apparent  $S_{275-295}$  decrease over time occurred in all the chambers (Fig. 4). The decrease in  $S_{275-295}$  was steeper at stations with higher pore-water DOC content. Thus, the fastest change in  $S_{275-295}$  occurred at St.1 ( $-0.016 \pm 0.017 \text{ nm}^{-1} \text{ d}^{-1}$ ) whereas slowest change was found at St.4 ( $-0.004 \pm 0.006 \text{ nm}^{-1} \text{ d}^{-1}$ ). (Fig.4, Table A1).

5 FDOM spectroscopy and PARAFAC analyses allowed four independent fluorescent components to be distinguished (Fig.6). FDOM components that are excited at UV and emit in the visible spectra were previously referred to as humic-like substances (e.g., Coble, 1996; Murphy et al., 2013, 2014; Loginova et al., 2016, and references therein). Here, two fluorescent components, FDOM component 1 (Comp.1) and FDOM component 2 (Comp.2), with excitation and emission (Ex/Em) of 370/464 nm and 290-325/400 nm, respectively, were assumed to be humic-like components (Fig. 6). Amino acid-like substances are a  
10 second group of well determined FDOM components (e.g., Coble, 1996; Murphy et al., 2013, 2014; Loginova et al., 2016, and references therein) corresponding to molecules that are excited and emit in the UV spectra. Thus, FDOM component 3 (Comp.3) and FDOM component 4 (Comp.4), with Ex/Em of 290/340(684) nm and 275/310(600) nm, respectively, were assumed to represent proteinaceous DOM (Fig. 6). During this study, humic-like components showed similar trends to DOC and  $a_{\text{CDOM}}(325)$  in the pore waters. Their fluorescence accumulated with sediment core depth and decreased offshore with a  
15 minimum fluorescence at St.4 (Fig.7). Amino acid-like Comp.3 and Comp.4, also accumulated in the pore waters, but were generally depleted throughout the sediment except for St.1, where their fluorescence reached max. 6 QSE and max. 1.7 QSE, respectively (Fig.7).

In the benthic chambers, all fluorescent component QSEs were nearly an order of magnitude lower than those in the pore waters. An apparent accumulation within chambers was observed for humic-like Comp.1 and Comp.2 and amino acid-like  
20 Comp.4 (Fig.8). Comp.3 displayed a slight apparent accumulation at the beginning of the sediment incubation followed by an apparent removal at a later stage (St.1, St.3, St.4 and St.6). Humic-like Comp.1, Comp.2 and amino acid-like Comp.4 displayed similar gradients among nearly all the stations of  $\sim 0.03$ ,  $0.06\text{--}0.08$  and  $0.03\text{--}0.04 \text{ QSE d}^{-1}$ , respectively. Exceptions were St.4 which displayed Comp.1, Comp.2 and Comp.4 gradients of 0.001, 0.04 and  $-0.005 \text{ QSE d}^{-1}$ , respectively; and St.1, where the gradients of Comp.2 and Comp.4 were  $\sim 0.04$  and  $\sim 0.09 \text{ QSE d}^{-1}$ , respectively (Table A1).

## 25 4 DISCUSSION

### 4.1 Spatial variability of the DOM fluxes at 12°S transect

Spatial variability of organic matter decomposition in sediments is a common feature in the world ocean (see Arndt et al., 2013, for overview). This variability is naturally attributed to the efficiency of vertical transfer of POM to the sediment (e.g. Seiter et al., 2004; Marsay et al., 2015; Engel et al., 2017). At 12°S, highest sedimentation rates, estimated via  $^{210}\text{Pb}_{xs}$  activity  
30 were reported for the inner shelf St.1 and St.2, while St.4 displayed the lowest sedimentation rates and pore water DOM concentrations possibly caused by an inhibition of particle settling by of bottom currents (Dale et al., 2015). The highest accumulation of POM at 12°S was also observed at St.1 and St.2 even though the organic carbon burial efficiency exhibited lower values at the inner shelf stations than the stations offshore (Dale et al., 2015).





Accordingly, pore water DOM optical properties reflect the "freshest" character of organic matter at St.1 and St.2, whereby  $S_{275-295}$  displayed similar properties to those in the water column (Fig. 4), an enrichment in protein-like DOM fluorescence (Fig. 7) and an enrichment in DON (Fig. 4). The data suggests that the inner shelf stations receive of the most labile POM, likely of proteinaceous origin (e.g. Faganeli and Herndl, 1991) compared to the outer shelf stations, which is likely being rapidly reworked into DOM at the inner shelf compared to the other sites.

Despite the highest sediment accumulation and POC mineralization rates at St.1 (Dale et al., 2015) and the "freshest" DOM character, the diffusive fluxes of DOC and DON here were not the highest on the transect even though pore waters showed elevated DOM levels (Fig. 9). This could be attributed to the spatially variable DOM recycling efficiencies and biogeochemical processes. For instance, denitrification and anammox were found to be the major processes of N cycling in the outer shelf and on the upper continental slope, whereas inner shelf stations, had elevated rates of DNRA, by sulphur-oxidising bacteria (Dale et al., 2016; Sommer et al., 2016). Whilst the linkage between microbial N turnover and DOM fluxes is unclear, it is noteworthy that the inner shelf sediments were covered with *Marthioplaca* mats that greatly affect the N and sulphur biogeochemical cycles and, potentially, DOM cycling and reactivity.

At St.2, DON accumulated to higher levels than DOC within the pore waters, leading to diffusive higher DON fluxes than those of DOC and extremely low DOC/DON ratios (Fig. A1). A so called "decoupling" between DOC and DON remineralization, leading to an accumulation of DON over DOC was previously ascribed to POM reactivity by e.g. Alkhatib et al. (2013). These authors suggested that the enzymatic hydrolysis of N-containing labile POM occurs at a higher rate than that of carbon-rich compounds, leading to lower DOC/DON ratios in the sediment pore waters. Furthermore, the dissolved by-products of bacterial activity are often found to be enriched in N, and therefore the sediments where microbial activity is pronounced show relatively low values of DOC/DON ratios (Burdige and Komada, 2015). Thus, glycine (DOC/DON=2) was suggested to preferentially accumulate as a result of microbial metabolism in mixed redox sediments (Burdige, 2002). Furthermore, bioturbation by macro-biota in oxygenated sediments is often associated with the accumulation of urea (DOC/DON=0.5) (Burdige and Gardner, 1998). Even though, the sediments off Peru are influenced by permanent OMZ, *Pleuroncodes monodon* are often found at 12°S (Kiko et al., 2015). However, given that retrieved sediment cores were apparently not bioturbated, an active remineralization of bio available organic matter by microbial communities within the sediment is more likely.

Furthermore, DOM itself may enter chemical reactions with hydrogen sulphide that is produced in large quantities at inner shelf stations (Schunck et al., 2013; Sommer et al., 2016). For instance, quinone structures can react with hydrogen sulphide, producing hydroquinones (Heitmann and Blodau, 2006), which may be further utilized by methanogenic degradation processes (Szewzyk et al., 1985). This could affect DOC and DON pore water concentrations and decrease the diffusive DOC flux over the diffusive DON flux.

The extreme accumulation of DON over the DOC in pore waters at St.2 and also St.1 seem to be hardly explainable with the organic N sources alone. Therefore, an additional inorganic N source might have been present and not captured by our analytical methods. For instance,  $\text{NO}_3^-$  that is present at high concentrations in intracellular vacuoles of *Marthioplaca* (Dale et al., 2016) could be leaked to the pore water during sediment handling and centrifugation. An ammonium oxidizing bacteria were shown previously to be able profiting from nitrous oxide, produced by denitrification (e.g. Kartal et al., 2013). Thus, the



production of  $\text{NH}_4^+$ , as a result of DNRA occurring at the inner shelf stations in combination to nitrous oxide production via denitrification occurring at outer shelf, may produce a convenient niche for anammox bacteria at the rim of the inner shelf at  $12^\circ\text{S}$ . The intermediate product of anammox, hydrazine (e.g. Kartal et al., 2013), may, in turn, accumulate in the inner space of anammox bacteria, and be released in the pore water samples as a consequence of the cell rupture induced by centrifugation.

5 However, the concentrations of those intermediate products are likely very small and may not explain elevated TDN values. Herewith, our arguments are speculative and the real mechanism behind the low DOC/DON remains obscure.

#### 4.2 Pore water DOM and its near-bottom utilization at the near coastal waters off Peru

In common understanding, production of DOM from POM degradation processes followed by slow microbial utilization of DOM (e.g. Burdige and Komada, 2015) causes an imbalance in production and degradation, resulting in a net accumulation

10 of DOM with sediment depth. This is, likely, due to an accumulation of biologically unavailable recalcitrant LMWDOM in the sediments produced by "microbial pump" (Burdige and Komada, 2015). Furthermore, physico-chemical processes, such as: 1) irreversible sorption onto particles, 2) aggregation (Liu and Lee, 2007; Arndt et al., 2013), 3) reactions of chelation and 4) co-precipitation (Lalonde et al., 2012), or 5) an inhibition of microbial activity (Emerson, 2013; Canfield, 1994; Aller and Aller, 1998) may contribute to the DOM accumulation in sediment pore waters. The observed accumulation of DOM

15 with depth in pore waters in this study (Fig. 3) agrees well previous observations (Burdige and Gardner, 1998; Komada et al., 2004; Chipman et al., 2010; Alkhatib et al., 2013) as well as with reported DOC concentrations in non-bioturbated anoxic sediments ( $\sim 1\text{--}3 \text{ mmol l}^{-1}$ ) (Burdige and Komada, 2015). The accumulation of humic-like fluorescence and its correlation with DOC concentrations (Comp.1,  $R=0.8$ ,  $n=0.86$ ,  $p<0.01$ ) as observed during our study has also been noted previously in marine sediments (e.g. Chen et al., 1993). The increase of the humic-like fluorescence with sediment depth is commonly

20 explained as a net production of LMW recalcitrant humic DOM and an increasing fraction of FDOM in the pore waters compared to the water column (Komada et al., 2004). The increase of  $S_{275-295}$  over sediment depth also indicated an increase of apparent molecular weight (Helms et al., 2008). This apparent increase in combination with the down-core enrichment in humic-like fluorescence suggests an accumulation of so-called polymeric LMW (pLMW) DOM. This may be formed via reactions of to geopolymerization (Hedges et al., 1988) or complexation (Finke et al., 2007), or due to formation of

25 supramolecular clusters via hydrogen bonding or hydrophobic interactions (e.g. Sutton and Sposito, 2005). The down-core accumulation of DON, as well as amino acid-like FDOM accumulation and its correlation to DOC (Comp.4,  $R=0.6$ ,  $n=0.86$ ,  $p<0.01$ ) suggest that proteinaceous DOM is also being produced during POM remineralization. Given that the second emission peaks of Comp.3 and Comp.4 displayed similar spectral characteristics to chl *a* and its auxiliary carotenoids (e.g. Wolf and Stevens, 1967), the protein-like FDOM components are likely products of phytoplankton debris recycling within the sediments.

30 Benthic DOM fluxes were previously shown to constitute an important fraction of the organic matter that escapes remineralization in the sediments (e.g. Ludwig et al., 1996; Burdige et al., 1999). Net *in situ* benthic DOC fluxes found during our study ( $-0.3\pm 0.9\text{--}2.3\pm 2.3 \text{ mmol m}^{-2}\text{d}^{-1}$ ) (Fig. 9) were comparable to previous estimates for shelf and continental slope sediments off coast of Peru and California, ranging from  $0.03\text{--}4.41 \text{ mmol m}^{-2}\text{d}^{-1}$  (see Burdige et al., 1992, 1999; Burdige and Komada, 2015, for full overview). However, the common assumption of linear accumulation of DOC and DON in benthic



chambers (Burdige et al., 1992; Burdige and Homstead, 1994; Burdige et al., 1999) over time was generally not met. We were able to trace the qualitative transformations of DOM in benthic chambers over the investigated time period by the changes in DOM optical properties. Thus, the decrease of  $S_{275-295}$  along with the enrichment in humic-like fluorescence over time may indicate an accumulation of LMW humic DOM components (Helms et al., 2008). A complex development of the amino acid-like fluorescence of Comp.3 and a drastic DON drawdown, resulting in increased DOC/DON ratios, in turn, may suggest that amino acid or proteinaceous DOM is potentially reworked within the benthic chambers during the investigated time period by microbial communities. Thus, the production of humic-like LMWDOM along with the utilization of proteinaceous DOM may indicate active microbial DOM utilization occurring in the near bottom waters (e.g. Alkhatib et al., 2013). Therefore our results from the benthic chambers suggest that the release of DOM to the water column may still stimulate its utilization by water-column microbial communities.

As stated previously, the rate of organic matter decomposition in sediments may be dependent not only on organic matter bio-availability (Canfield, 1994), but also on an inhibition of microbial activity (Aller and Aller, 1998), and availability of electron acceptors (Emerson, 2013; Canfield, 1994). We suggest that the availability of electron acceptors, such as  $\text{NO}_3^-$  and  $\text{NO}_2^-$  (Thomsen et al., 2016; Lüdke et al., 2019), in the water column above the sediments could stimulate near-bottom microbial communities to take up DOM that otherwise is recalcitrant. Furthermore, the formation of pLMWDOM due to geopolymerization, the formation of supra-molecules due to hydrogen bonding (Sutton and Sposito, 2005; Finke et al., 2007) or encapsulation by humic substances (e.g. Tomaszewski et al., 2011) may reduce accessibility of bio-available DOM compounds in sediments. Labile substances, such as amino acids and carbohydrates, may become unavailable for heterotrophic communities within the pore waters, resulting in DON accumulation with sediment depth. Subsequent release of pLMWDOM into the water column may lead to unfolding (solubilization) of those supra-molecules due to, e.g. the chaotropic effect of  $\text{NO}_3^-$  (e.g. Gibb and Gibb, 2011), and, consequently, increase DOM bio-availability for the near-bottom microbial communities.

Therefore, a non-conservative behaviour of DOC and DON in the BIGO chambers during the sediment enclosure might be a result of sediment release/microbial DOM consumption and reworking in the near bottom waters or the sediment—water column interface. In turn, DOM released by the sediment could potentially support an enhanced microbial abundance and carbon oxidation rates reported near the sediment on the 12°S transect (Maßmig et al., 2019a) and influence the activity of microbial mats that cover up to 100 % of the sediment surface at the inner shelf stations (Sommer et al., 2016). Furthermore, the DIC fluxes, evaluated in benthic lander systems (Dale et al., 2015) may include sediment release of DIC and the *in situ* DIC production by DOM remineralization. Given that the diffusive DOC fluxes, calculated in this study could represent up to ~53 % of the estimated DIC flux ( $J_{DIC}$ , A. Dale, unpubl.), while the net *in situ* benthic DOC fluxes could describe only up to ~28 % of  $J_{DIC}$ , POM remineralisation rates estimated from net *in situ* DIC flux will be subject to less bias, caused by the ignorance of DOM sediment release by previous studies. On the other hand, however, whether all the DOM utilization that takes place within benthic chambers in our study is actually bound to the sediment—water interface is not completely clear. Thus, the enclosure of the sediment over period of ~30 hrs may block out near bottom currents (e.g. Lüdke et al., 2019) and other mechanisms of lateral transport, e.g. eddies (Thomsen et al., 2016), that might influence the water column distribution of the freshly released from sediments DOM. For instance, Lüdke et al. (2019) reported near bottom poleward flow ranging from



0.1 to  $0.4 \text{ m s}^{-1}$ . That could imply, that, at stable flow, DOM, which have been released by the sediment, could be distributed along a distance of 10 to 40 km during the time equivalent to the time of sediment enclosure by BIGO chambers. Furthermore, Loginova et al. (2016) reported an apparent transport of similar by spectral properties to Comp.1 humic-like fluorescence to the surface waters at the beginning of their cruise. Therefore, DOM released to the bottom waters may be not limited to the sediment—water column interface, affecting whole water column biogeochemistry.

We suggest that the difference between the diffusive flux and net *in situ* flux could reflect the rate of microbial DOC utilization in the chamber water and/or surface sediment layer at each station. Thus, the rate of the microbial utilization at St.3–St.6 ranged from  $0.2$  to  $1.7 \text{ mmol m}^{-2} \text{ d}^{-1}$  (Fig. 9). These consumption rates could support a denitrification rate of  $0.2$ – $1.4 \text{ mmol m}^{-2} \text{ d}^{-1}$ , based on reaction stoichiometry reported by Prokopenko et al. (2011). These are comparable to denitrification ( $0.6 \pm 0.4 \text{ mmol m}^{-2} \text{ d}^{-1}$ ) and the total  $\text{N}_2$  efflux ( $\sim 1.2 \text{ mmol m}^{-2} \text{ d}^{-1}$ ) in anoxic sediments in the eastern tropical North Pacific off California (Prokopenko et al., 2011), to denitrification rates ( $0.2$ – $2 \text{ mmol m}^{-2} \text{ d}^{-1}$ ) in the eastern tropical North Atlantic off Mauritania (Dale et al., 2014) and to modelled denitrification rates ( $0.5$ – $1.1 \text{ mmol m}^{-2} \text{ d}^{-1}$ ) and  $\text{N}_2$  fluxes ( $0.8$ – $4.6 \text{ mmol m}^{-2} \text{ d}^{-1}$ ), observed along  $12^\circ\text{S}$  transect (Dale et al., 2016; Sommer et al., 2016). Furthermore, the estimated potential denitrification rates may be able to explain up to  $\sim 55\%$  of denitrification rates in the water column in the eastern tropical South Pacific ( $\sim 3 \text{ mmol m}^{-2} \text{ d}^{-1}$  Kalvelage et al., 2013), suggesting that sediment release of DOM may potentially serve as an important organic matter source for the water column N-loss.

## 5 Conclusions

Diffusive fluxes of DOC and DON displayed high spacial variability, which was likely caused by the quality of DOM supplied to the sediment and by differences in mechanisms of microbial metabolism with water depth, suggested in the previous studies. A general decrease of the net *in situ* DOC and DON fluxes, compared to the diffusive fluxes as well as an apparent steepening of  $S_{275-295}$  and accumulation of humic-like material within benthic chambers during the time of the sediment enclosure at all stations suggested that released to the water column DOM is being actively reworked near the sediment. The near-bottom remineralization of DOM is likely stimulated by high availability of strong electron acceptors, such as  $\text{NO}_3^-$  and  $\text{NO}_2^-$ , at the outer shelf and continental slope stations. The utilization of DOC released by the sediment, in turn, may account for denitrification rates, comparable to previously reported for the water column and sediments off Peru and other OMZs, suggesting sediment release to be an important source of bioavailable DOM.

*Data availability.* All the measured DOC concentrations,  $a_{\text{CDOM}(325)}$ ,  $S_{275-295}$  and QSE of fluorescent components will be available at pangaea.de with the link to the project: SFB754 upon publication



*Author contributions.* ANL designed the sampling strategy and analysed DOM samples. AWD collected samples at MUC and BIGO stations and provided data for calculation of fluxes, ST helped with water sampling, SS helped with the sampling strategy design and sampling and also provided all the facilities for sampling from BIGO landers, KW provided the initial idea for the research. ANL wrote the manuscript with contributions from AWD, FACLM, ST, SS, and AE.

5 *Competing interests.* The authors are not aware of competing interests of any sort for this research.

*Acknowledgements.* We are grateful to the chief scientists M. Dengler and ship and scientific crews of RV Meteor (cruises M136 and M137). J. Roa is acknowledged for DOC analyses. We are grateful to B. Domeyer, A. Bleyer, M. Türk and A. Beck for technical and logistical support, and to D. Clements and U. Schroller-Lomnitz for advice and data support.

This research has been supported by the Deutsche Forschungsgemeinschaft (DFG) grant no.: SFB754 “Climate-Biogeochemical Interactions in the Tropical Ocean” (miniproposal, B9) and funding provided by Inge-Lehmann-Fonds through GEOMAR Helmholtz Centre for Ocean Research awarded to ANL and by DFG Excellence cluster Future Ocean CP1403 “Transfer and remineralization of biogenic elements in the tropical oxygen minimum zones” awarded to FACLM.

10



## References

- Alkhatib, M., del Giorgio, P. A., Gelinas, Y., and Lehmann, M. F.: Benthic fluxes of dissolved organic nitrogen in the lower St. Lawrence estuary and implications for selective organic matter degradation, *Biogeosciences*, 10, 7609–7622, <https://doi.org/10.5194/bg-10-7609-2013>, <https://www.biogeosciences.net/10/7609/2013/>, 2013.
- 5 Aller, R. C. and Aller, J. Y.: The effect of biogenic irrigation intensity and solute exchange on diagenetic reaction rates in marine sediments, *Journal of Marine Research*, 56, 905–936, <https://doi.org/10.1357/002224098321667413>, <https://www.ingentaconnect.com/content/jmr/jmr/1998/00000056/00000004/art00008>, 1998.
- Arévalo-Martínez, D. L., Kock, A., Löscher, C. R., Schmitz, R. A., and Bange, H. W.: Massive nitrous oxide emissions from the tropical South Pacific Ocean, *Nature Geoscience*, 8, 530 EP –, <https://doi.org/10.1038/ngeo2469>, 2015.
- 10 Arndt, S., Jørgensen, B., LaRowe, D., Middelburg, J., Pancost, R., and Regnier, P.: Quantifying the degradation of organic matter in marine sediments: A review and synthesis, *Earth-Science Reviews*, 123, 53 – 86, <https://doi.org/10.1016/j.earscirev.2013.02.008>, <http://www.sciencedirect.com/science/article/pii/S0012825213000512>, 2013.
- Balch, J. and Guéguen, C.: Effects of molecular weight on the diffusion coefficient of aquatic dissolved organic matter and humic substances, *Chemosphere*, 119, 498 – 503, <https://doi.org/10.1016/j.chemosphere.2014.07.013>, <http://www.sciencedirect.com/science/article/pii/S0045653514008637>, 2015.
- 15 Belzile, C., Gibson, J. A. E., and Vincent, W. F.: Colored dissolved organic matter and dissolved organic carbon exclusion from lake ice: Implications for irradiance transmission and carbon cycling, *Limnology and Oceanography*, 47, 1283–1293, <https://doi.org/10.4319/lo.2002.47.5.1283>, <https://aslopubs.onlinelibrary.wiley.com/doi/abs/10.4319/lo.2002.47.5.1283>, 2002.
- Bricaud, A., Morel, A., and Prieur, L.: Absorption by dissolved organic matter of the sea (yellow substance) in the UV and visible domains I, *Limnology and Oceanography*, 26, 43–53, <https://doi.org/10.4319/lo.1981.26.1.0043>, <https://aslopubs.onlinelibrary.wiley.com/doi/abs/10.4319/lo.1981.26.1.0043>, 1981.
- 20 Burdige, D. J.: Chapter 13 - Sediment Pore Waters, in: *Biogeochemistry of Marine Dissolved Organic Matter*, edited by Hansell, D. A. and Carlson, C. A., pp. 611 – 663, Academic Press, San Diego, <https://doi.org/https://doi.org/10.1016/B978-012323841-2/50015-4>, <http://www.sciencedirect.com/science/article/pii/B9780123238412500154>, 2002.
- 25 Burdige, D. J. and Gardner, K. G.: Molecular weight distribution of dissolved organic carbon in marine sediment pore waters, *Marine Chemistry*, 62, 45 – 64, [https://doi.org/10.1016/S0304-4203\(98\)00035-8](https://doi.org/10.1016/S0304-4203(98)00035-8), <http://www.sciencedirect.com/science/article/pii/S0304420398000358>, 1998.
- Burdige, D. J. and Homstead, J.: Fluxes of dissolved organic carbon from Chesapeake Bay sediments, *Geochimica et Cosmochimica Acta*, 58, 3407 – 3424, [https://doi.org/10.1016/0016-7037\(94\)90095-7](https://doi.org/10.1016/0016-7037(94)90095-7), <http://www.sciencedirect.com/science/article/pii/0016703794900957>, 1994.
- 30 Burdige, D. J. and Komada, T.: Chapter 12 - Sediment Pore Waters, in: *Biogeochemistry of Marine Dissolved Organic Matter (Second Edition)*, edited by Hansell, D. A. and Carlson, C. A., pp. 535 – 577, Academic Press, Boston, second edition edn., <https://doi.org/10.1016/B978-0-12-405940-5.00012-1>, <http://www.sciencedirect.com/science/article/pii/B9780124059405000121>, 2015.
- Burdige, D. J., Alperin, M. J., Homstead, J., and Martens, C. S.: The Role of Benthic Fluxes of Dissolved Organic Carbon in Oceanic and Sedimentary Carbon Cycling, *Geophysical Research Letters*, 19, 1851–1854, <https://doi.org/10.1029/92GL02159>, <https://agupubs.onlinelibrary.wiley.com/doi/abs/10.1029/92GL02159>, 1992.
- 35



- Burdige, D. J., Berelson, W. M., Coale, K. H., McManus, J., and Johnson, K. S.: Fluxes of dissolved organic carbon from California continental margin sediments, *Geochimica et Cosmochimica Acta*, 63, 1507 – 1515, [https://doi.org/10.1016/S0016-7037\(99\)00066-6](https://doi.org/10.1016/S0016-7037(99)00066-6), <http://www.sciencedirect.com/science/article/pii/S0016703799000666>, 1999.
- Canfield, D. E.: Factors influencing organic carbon preservation in marine sediments, *Chemical Geology*, 114, 315 – 329, [https://doi.org/10.1016/0009-2541\(94\)90061-2](https://doi.org/10.1016/0009-2541(94)90061-2), <http://www.sciencedirect.com/science/article/pii/0009254194900612>, 1994.
- 5 Catalá, T. S., Álvarez Salgado, X. A., Otero, J., Iuculano, F., Companys, B., Horstkotte, B., Romera-Castillo, C., Nieto-Cid, M., Latasa, M., Morán, X. A. G., Gasol, J. M., Marrasé, C., Stedmon, C. A., and Reche, I.: Drivers of fluorescent dissolved organic matter in the global epipelagic ocean, *Limnology and Oceanography*, 61, 1101–1119, <https://doi.org/10.1002/lno.10281>, <https://aslopubs.onlinelibrary.wiley.com/doi/abs/10.1002/lno.10281>, 2016.
- 10 Chen, M., Kim, J.-H., Nam, S.-I., Niessen, F., Hong, W.-L., Kang, M.-H., and Hur, J.: Production of fluorescent dissolved organic matter in Arctic Ocean sediments, *Scientific Reports*, 6, 39 213 EP –, <https://doi.org/10.1038/srep39213>, article, 2016.
- Chen, R. F., Bada, J. L., and Suzuki, Y.: The relationship between dissolved organic carbon (DOC) and fluorescence in anoxic marine porewaters: Implications for estimating benthic DOC fluxes, *Geochimica et Cosmochimica Acta*, 57, 2149 – 2153, [https://doi.org/10.1016/0016-7037\(93\)90102-3](https://doi.org/10.1016/0016-7037(93)90102-3), <http://www.sciencedirect.com/science/article/pii/0016703793901023>, 1993.
- 15 Chipman, L., Podgorski, D., Green, S., Kostka, J., Cooper, W., and Huettel, M.: Decomposition of plankton-derived dissolved organic matter in permeable coastal sediments, *Limnology and Oceanography*, 55, 857–871, <https://doi.org/10.4319/lo.2010.55.2.0857>, <https://aslopubs.onlinelibrary.wiley.com/doi/abs/10.4319/lo.2010.55.2.0857>, 2010.
- Coble, P. G.: Characterization of marine and terrestrial DOM in seawater using excitation-emission matrix spectroscopy, *Marine Chemistry*, 51, 325 – 346, [https://doi.org/10.1016/0304-4203\(95\)00062-3](https://doi.org/10.1016/0304-4203(95)00062-3), <http://www.sciencedirect.com/science/article/pii/0304420395000623>, 20 1996.
- Dale, A., Sommer, S., Ryabenko, E., Noffke, A., Bohlen, L., Wallmann, K., Stolpovsky, K., Greinert, J., and Pfannkuche, O.: Benthic nitrogen fluxes and fractionation of nitrate in the Mauritanian oxygen minimum zone (Eastern Tropical North Atlantic), *Geochimica et Cosmochimica Acta*, 134, 234 – 256, <https://doi.org/10.1016/j.gca.2014.02.026>, <http://www.sciencedirect.com/science/article/pii/S0016703714001331>, 2014.
- 25 Dale, A., Sommer, S., Lomnitz, U., Bourbonnais, A., and Wallmann, K.: Biological nitrate transport in sediments on the Peruvian margin mitigates benthic sulfide emissions and drives pelagic N loss during stagnation events, *Deep Sea Research Part I: Oceanographic Research Papers*, 112, 123 – 136, <https://doi.org/10.1016/j.dsr.2016.02.013>, <http://www.sciencedirect.com/science/article/pii/S0967063715301308>, 2016.
- Dale, A. W., Sommer, S., Lomnitz, U., Montes, I., Treude, T., Liebetrau, V., Gier, J., Hensen, C., Dengler, M., Stolpovsky, K., Bryant, L. D., 30 and Wallmann, K.: Organic carbon production, mineralisation and preservation on the Peruvian margin, *Biogeosciences*, 12, 1537–1559, <https://doi.org/10.5194/bg-12-1537-2015>, <https://www.biogeosciences.net/12/1537/2015/>, 2015.
- Del Vecchio, R. and Blough, N. V.: On the Origin of the Optical Properties of Humic Substances, *Environmental Science & Technology*, 38, 3885–3891, <https://doi.org/10.1021/es049912h>, <https://doi.org/10.1021/es049912h>, 2004.
- Demaison, G. and Moore, G.: Anoxic environments and oil source bed genesis, *Organic Geochemistry*, 2, 9 – 31, [https://doi.org/10.1016/0146-6380\(80\)90017-0](https://doi.org/10.1016/0146-6380(80)90017-0), <http://www.sciencedirect.com/science/article/pii/0146638080900170>, 1980.
- Dickson, A. G., Sabine, C. L., and Christian, J. R.: Guide to best practices for ocean CO<sub>2</sub> measurements, 2007.
- Emerson, S.: Organic Carbon Preservation in Marine Sediments, pp. 78–87, American Geophysical Union (AGU), <https://doi.org/10.1029/GM032p0078>, <https://agupubs.onlinelibrary.wiley.com/doi/abs/10.1029/GM032p0078>, 2013.



- Engel, A. and Galgani, L.: The organic sea-surface microlayer in the upwelling region off the coast of Peru and potential implications for air–sea exchange processes, *Biogeosciences*, 13, 989–1007, <https://doi.org/10.5194/bg-13-989-2016>, <https://www.biogeosciences.net/13/989/2016/>, 2016.
- 5 Engel, A., Wagner, H., Le Moigne, F. A. C., and Wilson, S. T.: Particle export fluxes to the oxygen minimum zone of the eastern tropical North Atlantic, *Biogeosciences*, 14, 1825–1838, <https://doi.org/10.5194/bg-14-1825-2017>, <https://www.biogeosciences.net/14/1825/2017/>, 2017.
- Faganeli, J. and Herndl, G.: Behaviour of Dissolved Organic Matter in Pore Waters of Near-Shore Marine Sediments, in: Diversity of Environmental Biogeochemistry, edited by Berthelin, J., vol. 6 of *Developments in Geochemistry*, pp. 157 – 170, Elsevier, <https://doi.org/10.1016/B978-0-444-88900-3.50020-5>, <http://www.sciencedirect.com/science/article/pii/B9780444889003500205>, 1991.
- 10 Finke, N., Hoehler, T. M., and Jørgensen, B. B.: Hydrogen ‘leakage’ during methanogenesis from methanol and methylamine: implications for anaerobic carbon degradation pathways in aquatic sediments, *Environmental Microbiology*, 9, 1060–1071, <https://doi.org/10.1111/j.1462-2920.2007.01248.x>, <https://onlinelibrary.wiley.com/doi/abs/10.1111/j.1462-2920.2007.01248.x>, 2007.
- 15 Gibb, C. L. D. and Gibb, B. C.: Anion Binding to Hydrophobic Concavity Is Central to the Salting-in Effects of Hofmeister Chaotropes, *Journal of the American Chemical Society*, 133, 7344–7347, <https://doi.org/10.1021/ja202308n>, <https://doi.org/10.1021/ja202308n>, 2011.
- Glock, N., Roy, A.-S., Romero, D., Wein, T., Weissenbach, J., Revsbech, N. P., Høglund, S., Clemens, D., Sommer, S., and Dagan, T.: Metabolic preference of nitrate over oxygen as an electron acceptor in foraminifera from the Peruvian oxygen minimum zone, *Proceedings of the National Academy of Sciences*, 116, 2860–2865, <https://doi.org/10.1073/pnas.1813887116>, <https://www.pnas.org/content/116/8/2860>, 2019.
- 20 Hansen, H. and Koroleff, F.: Determination of nutrients, chap. 10, pp. 159–228, John Wiley and Sons, 3 edn., <https://doi.org/10.1002/9783527613984.ch10>, 2007.
- Hedges, J. I., Clark, W. A., and Come, G. L.: Fluxes and reactivities of organic matter in a coastal marine bay, *Limnology and Oceanography*, 33, 1137–1152, <https://doi.org/10.4319/lo.1988.33.5.1137>, <https://aslopubs.onlinelibrary.wiley.com/doi/abs/10.4319/lo.1988.33.5.1137>, 1988.
- 25 Heitmann, T. and Blodau, C.: Oxidation and incorporation of hydrogen sulfide by dissolved organic matter, *Chemical Geology*, 235, 12 – 20, <https://doi.org/10.1016/j.chemgeo.2006.05.011>, <http://www.sciencedirect.com/science/article/pii/S0009254106002737>, 2006.
- Helms, J. R., Stubbins, A., Ritchie, J. D., Minor, E. C., Kieber, D. J., and Mopper, K.: Absorption spectral slopes and slope ratios as indicators of molecular weight, source, and photobleaching of chromophoric dissolved organic matter, *Limnology and Oceanography*, 53, 955–969, <https://doi.org/10.4319/lo.2008.53.3.0955>, <https://aslopubs.onlinelibrary.wiley.com/doi/abs/10.4319/lo.2008.53.3.0955>, 2008.
- 30 Jørgensen, L., Stedmon, C. A., Kragh, T., Markager, S., Middelboe, M., and Søndergaard, M.: Global trends in the fluorescence characteristics and distribution of marine dissolved organic matter, *Marine Chemistry*, 126, 139 – 148, <https://doi.org/10.1016/j.marchem.2011.05.002>, <http://www.sciencedirect.com/science/article/pii/S0304420311000569>, 2011.
- 35 Kalvelage, T., Lavik, G., Lam, P., Contreras, S., Arteaga, L., Löscher, C. R., Oschlies, A., Paulmier, A., Stramma, L., and Kuypers, M. M.: Nitrogen cycling driven by organic matter export in the South Pacific oxygen minimum zone, *Nature Geoscience*, 6, 228 EP –, <https://doi.org/10.1038/ngeo1739>, article, 2013.





- Kartal, B., de Almeida, N. M., Maalcke, W. J., Op den Camp, H. J., Jetten, M. S., and Keltjens, J. T.: How to make a living from anaerobic ammonium oxidation, *FEMS Microbiology Reviews*, 37, 428–461, <https://doi.org/10.1111/1574-6976.12014>, <https://doi.org/10.1111/1574-6976.12014>, 2013.
- Keeling, R. F., Körtzinger, A., and Gruber, N.: Ocean Deoxygenation in a Warming World, *Annual Review of Marine Science*, 2, 199–229, <https://doi.org/10.1146/annurev.marine.010908.163855>, <https://doi.org/10.1146/annurev.marine.010908.163855>, PMID: 21141663, 2010.
- 5 Kiko, R., Hauss, H., Dengler, M., Sommer, S., and Melzner, F.: The squat lobster *Pleuroncodes monodon* tolerates anoxic “dead zone” conditions off Peru, *Marine Biology*, 162, 1913–1921, <https://doi.org/10.1007/s00227-015-2709-6>, <https://doi.org/10.1007/s00227-015-2709-6>, 2015.
- Komada, T., Reimers, C. E., Luther, G. W., and Burdige, D. J.: Factors affecting dissolved organic matter dynamics in mixed-redox to anoxic coastal sediments, *Geochimica et Cosmochimica Acta*, 68, 4099 – 4111, <https://doi.org/10.1016/j.gca.2004.04.005>, <http://www.sciencedirect.com/science/article/pii/S0016703704002789>, 2004.
- Komada, T., Burdige, D. J., Li, H.-L., Magen, C., Chanton, J. P., and Cada, A. K.: Organic matter cycling across the sulfate-methane transition zone of the Santa Barbara Basin, California Borderland, *Geochimica et Cosmochimica Acta*, 176, 259 – 278, <https://doi.org/10.1016/j.gca.2015.12.022>, <http://www.sciencedirect.com/science/article/pii/S0016703715007164>, 2016.
- 15 Lalonde, K., Mucci, A., Ouellet, A., and Gélinas, Y.: Preservation of organic matter in sediments promoted by iron, *Nature*, 483, 198–200, <https://doi.org/10.1038/nature10855>, <https://doi.org/10.1038/nature10855>, 2012.
- Lavery, P. S., Oldham, C. E., and Ghisalberti, M.: The use of Fick’s First Law for predicting porewater nutrient fluxes under diffusive conditions, *Hydrological Processes*, 15, 2435–2451, <https://doi.org/10.1002/hyp.297>, <https://onlinelibrary.wiley.com/doi/abs/10.1002/hyp.297>, 2001.
- 20 Le Moigne, F. A. C., Cisternas-Novoa, C., Piontek, J., Maßmig, M., and Engel, A.: On the effect of low oxygen concentrations on bacterial degradation of sinking particles, *Scientific Reports*, 7, 16722, <https://doi.org/10.1038/s41598-017-16903-3>, <https://doi.org/10.1038/s41598-017-16903-3>, 2017.
- Levin, L., Gutiérrez, D., Rathburn, A., Neira, C., Sellanes, J., Muñoz, P., Gallardo, V., and Salamanca, M.: Benthic processes on the Peru margin: a transect across the oxygen minimum zone during the 1997–98 El Niño, *Progress in Oceanography*, 53, 1 – 27, [https://doi.org/https://doi.org/10.1016/S0079-6611\(02\)00022-8](https://doi.org/https://doi.org/10.1016/S0079-6611(02)00022-8), <http://www.sciencedirect.com/science/article/pii/S0079661102000228>, 2002.
- 25 Liu, Z. and Lee, C.: The role of organic matter in the sorption capacity of marine sediments, *Marine Chemistry*, 105, 240 – 257, <https://doi.org/https://doi.org/10.1016/j.marchem.2007.02.006>, <http://www.sciencedirect.com/science/article/pii/S0304420307000527>, 2007.
- 30 Loginova, A. N., Thomsen, S., and Engel, A.: Chromophoric and fluorescent dissolved organic matter in and above the oxygen minimum zone off Peru, *Journal of Geophysical Research: Oceans*, 121, 7973–7990, <https://doi.org/10.1002/2016JC011906>, <https://agupubs.onlinelibrary.wiley.com/doi/abs/10.1002/2016JC011906>, 2016.
- Loginova, A. N., Thomsen, S., Dengler, M., Lüdke, J., and Engel, A.: Diapycnal dissolved organic matter supply into the upper Peruvian oxycline, *Biogeosciences*, 16, 2033–2047, <https://doi.org/10.5194/bg-16-2033-2019>, <https://www.biogeosciences.net/16/2033/2019/>, 2019.
- 35 Lüdke, J., Dengler, M., Sommer, S., Clemens, D., Thomsen, S., Krahnemann, G., Dale, A. W., Achterberg, E. P., and Visbeck, M.: Influence of intraseasonal eastern boundary circulation variability on hydrography and biogeochemistry off Peru, *Ocean Science Discussions*, 2019, 1–31, <https://doi.org/10.5194/os-2019-93>, <https://www.ocean-sci-discuss.net/os-2019-93/>, 2019.



- Ludwig, W., Probst, J.-L., and Kempe, S.: Predicting the oceanic input of organic carbon by continental erosion, *Global Biogeochemical Cycles*, 10, 23–41, <https://doi.org/10.1029/95GB02925>, <https://agupubs.onlinelibrary.wiley.com/doi/abs/10.1029/95GB02925>, 1996.
- Marsay, C. M., Sanders, R. J., Henson, S. A., Pabortsava, K., Achterberg, E. P., and Lampitt, R. S.: Attenuation of sinking particulate organic carbon flux through the mesopelagic ocean, *Proceedings of the National Academy of Sciences*, 112, 1089–1094, <https://doi.org/10.1073/pnas.1415311112>, <https://www.pnas.org/content/112/4/1089>, 2015.
- Maßmig, M., Lüdke, J., Krahnemann, G., and Engel, A.: High bacterial organic carbon uptake in the Eastern Tropical South Pacific oxygen minimum zone, *Biogeosciences Discussions*, 2019, 1–26, <https://doi.org/10.5194/bg-2019-237>, <https://www.biogeosciences-discuss.net/bg-2019-237/>, 2019a.
- Maßmig, M., Piontek, J., Le Moigne, F., Cisternas-Novoa, C., and Engel, A.: Potential role of oxygen and inorganic nutrients on microbial carbon turnover in the Baltic Sea, *Aquatic Microbial Ecology*, 83, 95–108, <https://doi.org/10.3354/ame01902>, <https://www.int-res.com/abstracts/ame/v83/n1/p95-108/>, 2019b.
- Moran, M. A. and Zepp, R. G.: Role of photoreactions in the formation of biologically labile compounds from dissolved organic matter, *Limnology and Oceanography*, 42, 1307–1316, <https://doi.org/10.4319/lo.1997.42.6.1307>, <https://aslopubs.onlinelibrary.wiley.com/doi/abs/10.4319/lo.1997.42.6.1307>, 1997.
- Murphy, K. R., Stedmon, C. A., Graeber, D., and Bro, R.: Fluorescence spectroscopy and multi-way techniques. PARAFAC, *Anal. Methods*, 5, 6557–6566, <https://doi.org/10.1039/C3AY41160E>, <http://dx.doi.org/10.1039/C3AY41160E>, 2013.
- Murphy, K. R., Stedmon, C. A., Wenig, P., and Bro, R.: OpenFluor– an online spectral library of auto-fluorescence by organic compounds in the environment, *Anal. Methods*, 6, 658–661, <https://doi.org/10.1039/C3AY41935E>, 10.1039/C3AY41935E, 2014.
- Nelson, N. B. and Siegel, D. A.: The Global Distribution and Dynamics of Chromophoric Dissolved Organic Matter, *Annual Review of Marine Science*, 5, 447–476, <https://doi.org/10.1146/annurev-marine-120710-100751>, <https://doi.org/10.1146/annurev-marine-120710-100751>, PMID: 22809178, 2013.
- Pantoja, S., Rossel, P., Castro, R., Cuevas, L. A., Daneri, G., and Córdova, C.: Microbial degradation rates of small peptides and amino acids in the oxygen minimum zone of Chilean coastal waters, *Deep Sea Research Part II: Topical Studies in Oceanography*, 56, 1055 – 1062, <https://doi.org/10.1016/j.dsr2.2008.09.007>, <http://www.sciencedirect.com/science/article/pii/S0967064508003251>, the *Oceanography of the Eastern South Pacific II: The Oxygen Minimum Zone*, 2009.
- Pennington, J. T., Mahoney, K. L., Kuwahara, V. S., Kolber, D. D., Calienes, R., and Chavez, F. P.: Primary production in the eastern tropical Pacific: A review, *Progress in Oceanography*, 69, 285 – 317, <https://doi.org/10.1016/j.pocean.2006.03.012>, <http://www.sciencedirect.com/science/article/pii/S0079661106000358>, a Review of Eastern Tropical Pacific Oceanography, 2006.
- Prokopenko, M., Sigman, D., Berelson, W., Hammond, D., Barnett, B., Chong, L., and Townsend-Small, A.: Denitrification in anoxic sediments supported by biological nitrate transport, *Geochimica et Cosmochimica Acta*, 75, 7180 – 7199, <https://doi.org/10.1016/j.gca.2011.09.023>, <http://www.sciencedirect.com/science/article/pii/S0016703711005448>, 2011.
- Rodríguez-Morata, C., Díaz, H. F., Ballesteros-Canovas, J. A., Rohrer, M., and Stoffel, M.: The anomalous 2017 coastal El Niño event in Peru, *Climate Dynamics*, 52, 5605–5622, <https://doi.org/10.1007/s00382-018-4466-y>, <https://doi.org/10.1007/s00382-018-4466-y>, 2019.
- Schunck, H., Lavik, G., Desai, D. K., Großkopf, T., Kalvelage, T., Löscher, C. R., Paulmier, A., Contreras, S., Siegel, H., Holtappels, M., Rosenstiel, P., Schilhabel, M. B., Graco, M., Schmitz, R. A., Kuypers, M. M. M., and LaRoche, J.: Giant Hydrogen Sulfide Plume in the Oxygen Minimum Zone off Peru Supports Chemolithoautotrophy, *PLOS ONE*, 8, 1–18, <https://doi.org/10.1371/journal.pone.0068661>, <https://doi.org/10.1371/journal.pone.0068661>, 2013.



- Seiter, K., Hensen, C., Schröter, J., and Zabel, M.: Organic carbon content in surface sediments—defining regional provinces, *Deep Sea Research Part I: Oceanographic Research Papers*, 51, 2001 – 2026, <https://doi.org/10.1016/j.dsr.2004.06.014>, <http://www.sciencedirect.com/science/article/pii/S0967063704001384>, 2004.
- Smith, D. C., Simon, M., Alldredge, A. L., and Azam, F.: Intense hydrolytic enzyme activity on marine aggregates and implications for rapid particle dissolution, *Nature*, 359, 139–142, <https://doi.org/10.1038/359139a0>, <https://doi.org/10.1038/359139a0>, 1992.
- 5 Sommer, S., Türk, M., Kriwanek, S., and Pfannkuche, O.: Gas exchange system for extended in situ benthic chamber flux measurements under controlled oxygen conditions: First application—Sea bed methane emission measurements at Captain Arutyunov mud volcano, *Limnology and Oceanography: Methods*, 6, 23–33, <https://doi.org/10.4319/lom.2008.6.23>, <https://aslopubs.onlinelibrary.wiley.com/doi/abs/10.4319/lom.2008.6.23>, 2008.
- 10 Sommer, S., Gier, J., Treude, T., Lomnitz, U., Dengler, M., Cardich, J., and Dale, A.: Depletion of oxygen, nitrate and nitrite in the Peruvian oxygen minimum zone cause an imbalance of benthic nitrogen fluxes, *Deep Sea Research Part I: Oceanographic Research Papers*, 112, 113 – 122, <https://doi.org/10.1016/j.dsr.2016.03.001>, <http://www.sciencedirect.com/science/article/pii/S0967063715300819>, 2016.
- Stedmon, C. A. and Bro, R.: Characterizing dissolved organic matter fluorescence with parallel factor analysis: a tutorial, *Limnology and Oceanography: Methods*, 6, 572–579, <https://doi.org/10.4319/lom.2008.6.572>, <https://aslopubs.onlinelibrary.wiley.com/doi/abs/10.4319/lom.2008.6.572>, 2008.
- 15 Stramma, L., Hüttl, S., and Schafstall, J.: Water masses and currents in the upper tropical northeast Atlantic off northwest Africa, *Journal of Geophysical Research: Oceans*, 110, <https://doi.org/10.1029/2005JC002939>, <https://agupubs.onlinelibrary.wiley.com/doi/abs/10.1029/2005JC002939>, 2005.
- Stramma, L., Johnson, G. C., Sprintall, J., and Mohrholz, V.: Expanding Oxygen-Minimum Zones in the Tropical Oceans, *Science*, 320, 655–658, <https://doi.org/10.1126/science.1153847>, <https://science.sciencemag.org/content/320/5876/655>, 2008.
- 20 Sutton, R. and Sposito, G.: Molecular Structure in Soil Humic Substances: The New View, *Environmental Science & Technology*, 39, 9009–9015, <https://doi.org/10.1021/es050778q>, <https://doi.org/10.1021/es050778q>, 2005.
- Szewzyk, U., Szewzyk, R., and Schink, B.: Methanogenic degradation of hydroquinone and catechol via reductive dehydroxylation to phenol, *FEMS Microbiology Letters*, 31, 79 – 87, [https://doi.org/10.1016/0378-1097\(85\)90003-5](https://doi.org/10.1016/0378-1097(85)90003-5), <http://www.sciencedirect.com/science/article/pii/0378109785900035>, 1985.
- 25 Thomsen, S., Kanzow, T., Krahnemann, G., Greatbatch, R. J., Dengler, M., and Lavik, G.: The formation of a subsurface anticyclonic eddy in the Peru-Chile Undercurrent and its impact on the near-coastal salinity, oxygen, and nutrient distributions, *Journal of Geophysical Research: Oceans*, 121, 476–501, <https://doi.org/10.1002/2015JC010878>, <https://agupubs.onlinelibrary.wiley.com/doi/abs/10.1002/2015JC010878>, 2016.
- 30 Tomaszewski, J. E., Schwarzenbach, R. P., and Sander, M.: Protein Encapsulation by Humic Substances, *Environmental Science & Technology*, 45, 6003–6010, <https://doi.org/10.1021/es200663h>, <https://doi.org/10.1021/es200663h>, 2011.
- Ullman, W. J. and Aller, R. C.: Diffusion coefficients in nearshore marine sediments1, *Limnology and Oceanography*, 27, 552–556, <https://doi.org/10.4319/lo.1982.27.3.0552>, <https://aslopubs.onlinelibrary.wiley.com/doi/abs/10.4319/lo.1982.27.3.0552>, 1982.
- Wolf, F. T. and Stevens, M. V.: THE FLUORESCENCE OF CAROTENOIDS, *Photochemistry and Photobiology*, 6, 597–599, <https://doi.org/10.1111/j.1751-1097.1967.tb08761.x>, <https://onlinelibrary.wiley.com/doi/abs/10.1111/j.1751-1097.1967.tb08761.x>, 1967.
- 35 Yang, L., Choi, J. H., and Hur, J.: Benthic flux of dissolved organic matter from lake sediment at different redox conditions and the possible effects of biogeochemical processes, *Water Research*, 61, 97 – 107, <https://doi.org/https://doi.org/10.1016/j.watres.2014.05.009>, <http://www.sciencedirect.com/science/article/pii/S0043135414003546>, 2014.

<https://doi.org/10.5194/bg-2019-489>  
Preprint. Discussion started: 28 January 2020  
© Author(s) 2020. CC BY 4.0 License.



Zsolnay, A., Baigar, E., Jimenez, M., Steinweg, B., and Saccomandi, F.: Differentiating with fluorescence spectroscopy the sources of dissolved organic matter in soils subjected to drying, *Chemosphere*, 38, 45 – 50, [https://doi.org/https://doi.org/10.1016/S0045-6535\(98\)00166-0](https://doi.org/https://doi.org/10.1016/S0045-6535(98)00166-0), <http://www.sciencedirect.com/science/article/pii/S0045653598001660>, 1999.

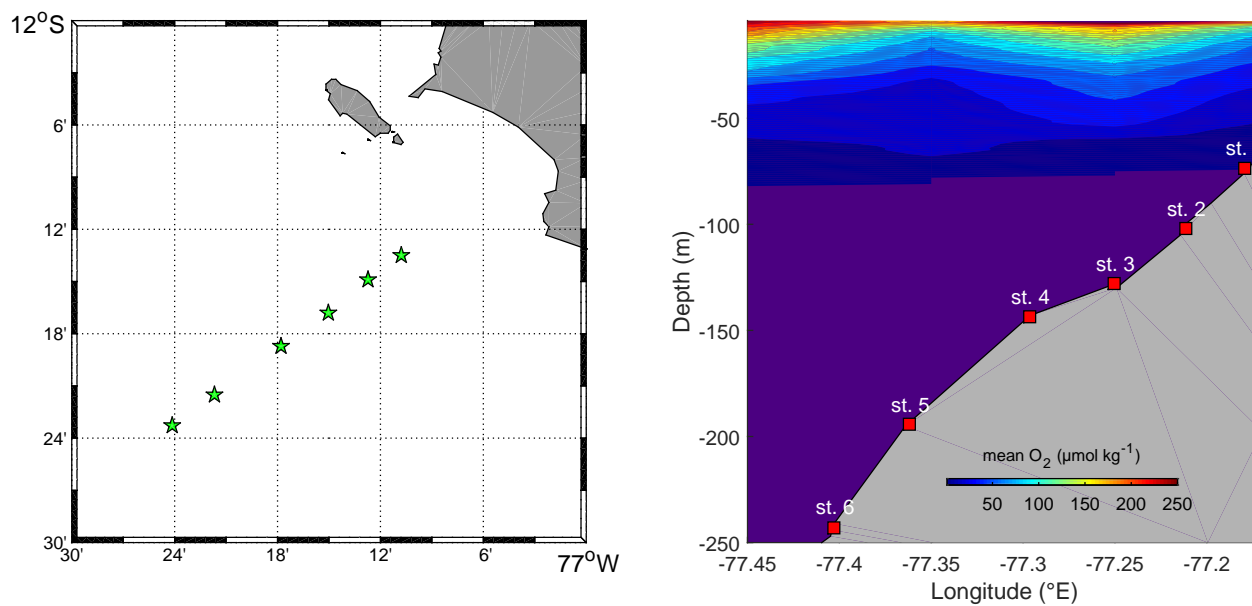


**Figure 1.** Distribution of sampling stations. Right: mean oxygen plot (the  $O_2$  values were averaged over 1m depth and  $0.1^\circ$  longitude intervals). The indigo colour represents values below  $1 \mu\text{mol kg}^{-1}$

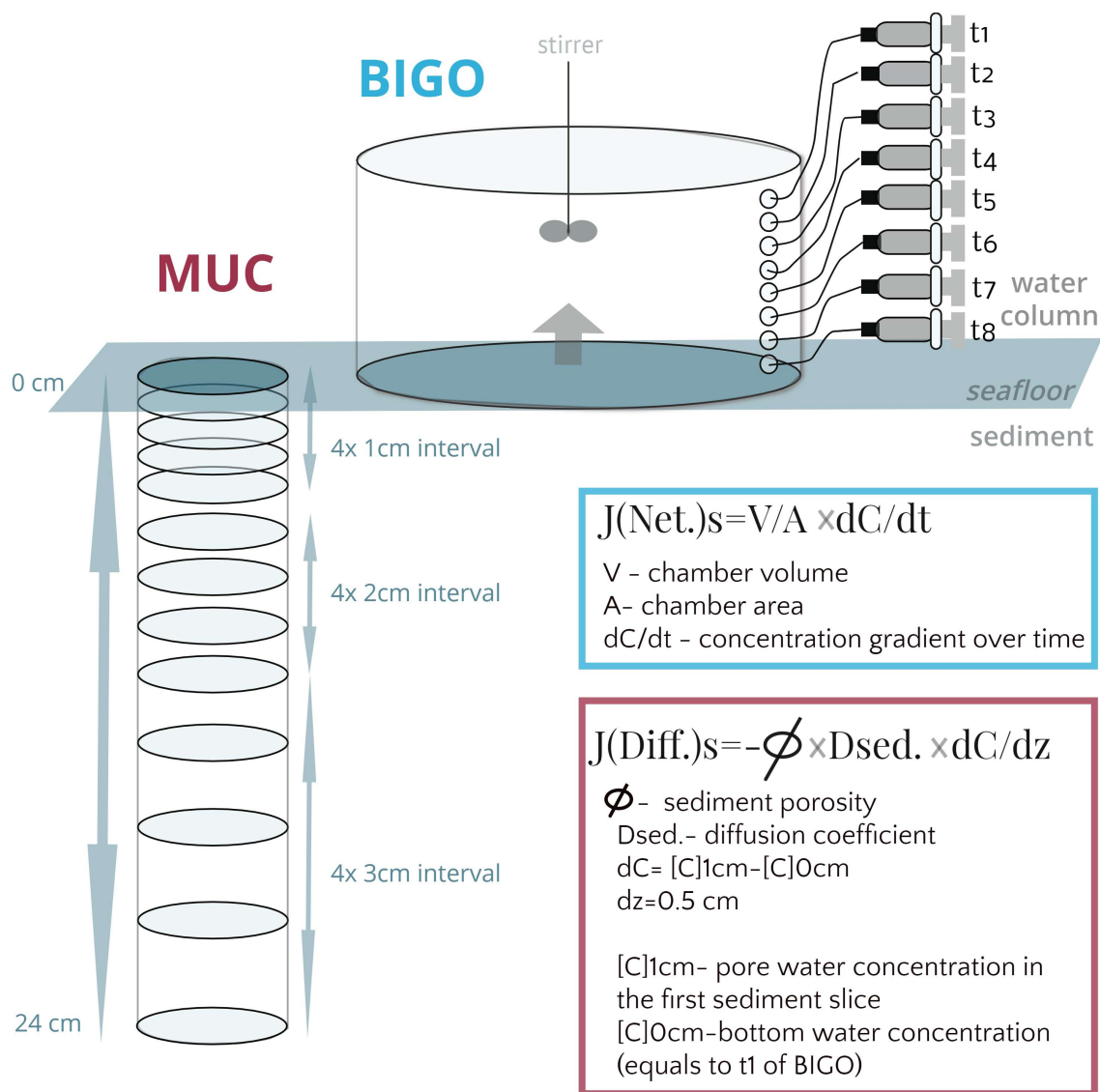


**Figure 2.** Schematic representation of a sediment core taken by MUC and a BIGO chamber. Each sediment core was sliced over 1–3 cm intervals to get average resolution of 12 samples per sediment core. A concentration gradient of solutes was obtained as a difference of the pore water concentration of a solute, analysed at the first sediment slice and bottom water solute concentration, that was assumed equal to the solute concentration measured in the corresponding BIGO chamber at time-point  $t_1$ . Each BIGO chamber was deployed over the period of ~ 32 hrs, during that time samples were retrieved sequentially at time points of ~0.2, 4, 9, 12, 17, 25 and ~ 30 hrs using glass air and water tight 40 ml syringes. The concentration gradient of a solute over time was obtained by fitting a linear regression to the time—concentration plot, as it is shown on Fig 4.

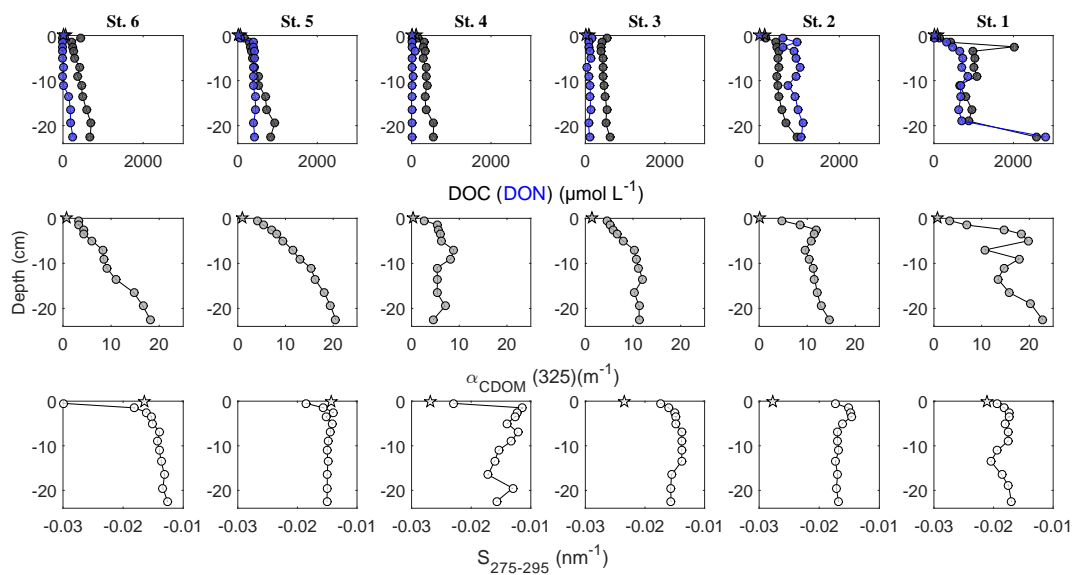


**Figure 3.** Pore water DOC (dark grey symbols), DON (blue symbols),  $\alpha_{\text{CDOM}}(325)$  (light grey symbols) and  $S_{275-295}$  (white symbols) distribution within the sediments: depth profiles. Circles represent concentration/value, measured in the pore water sample, pentagons represent the initial concentration/value of the bottom water.

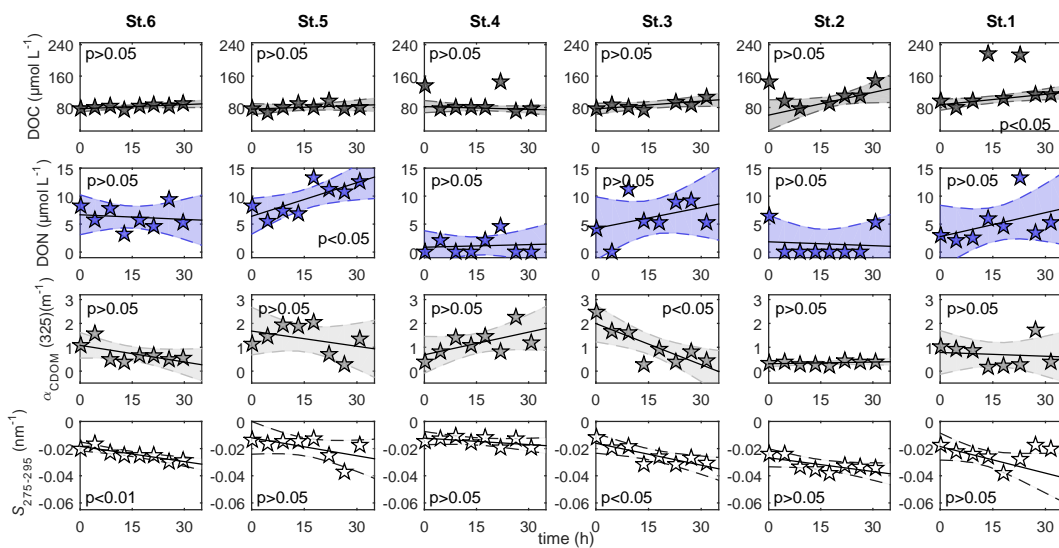


**Figure 4.** Distribution of DOC and CDOM parameters,  $\alpha_{\text{CDOM}}(325)$  and  $S_{275-295}$ , measured in BIGO chambers over time. Polynomial fit (1st order) was used for linear regression analyses:  $t_0$  and data included in brackets were excluded from the analyses.



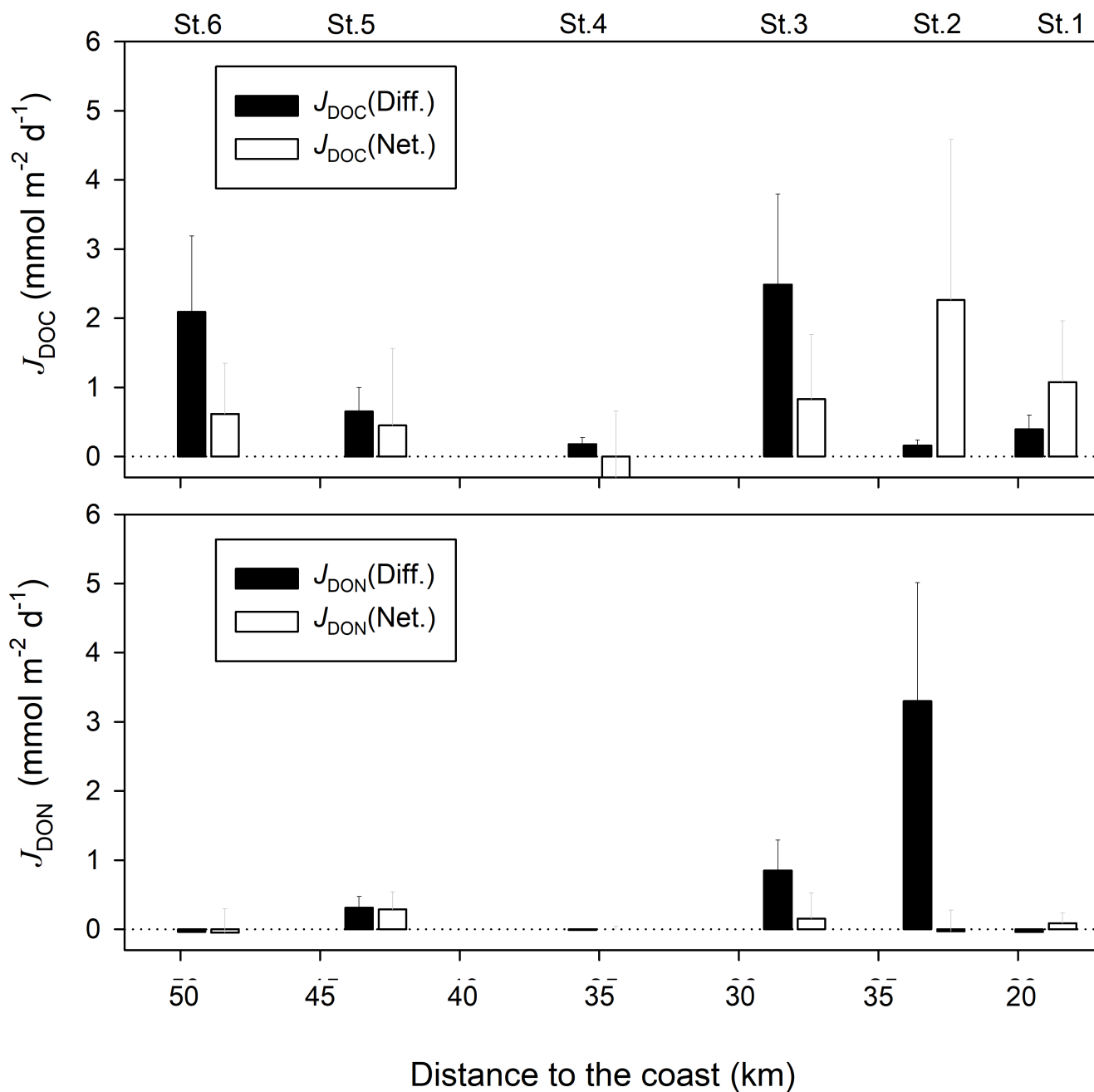


**Figure 5.** Diffusive and *in situ* net DOC (upper panel) and DON (lower panel) fluxes, evaluated at 12°S transect during this study.

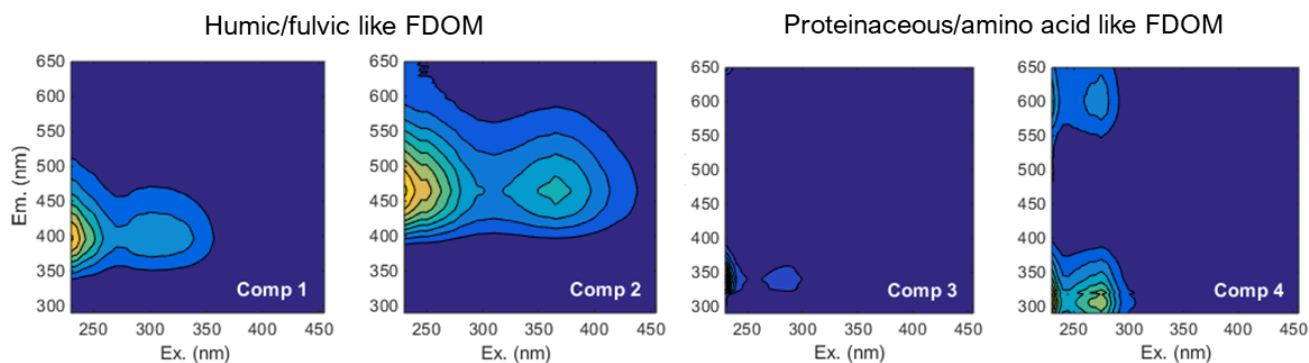


**Figure 6.** Four-components, which were found and validated by PARAFAC analyses after Murphy et al.(2013)

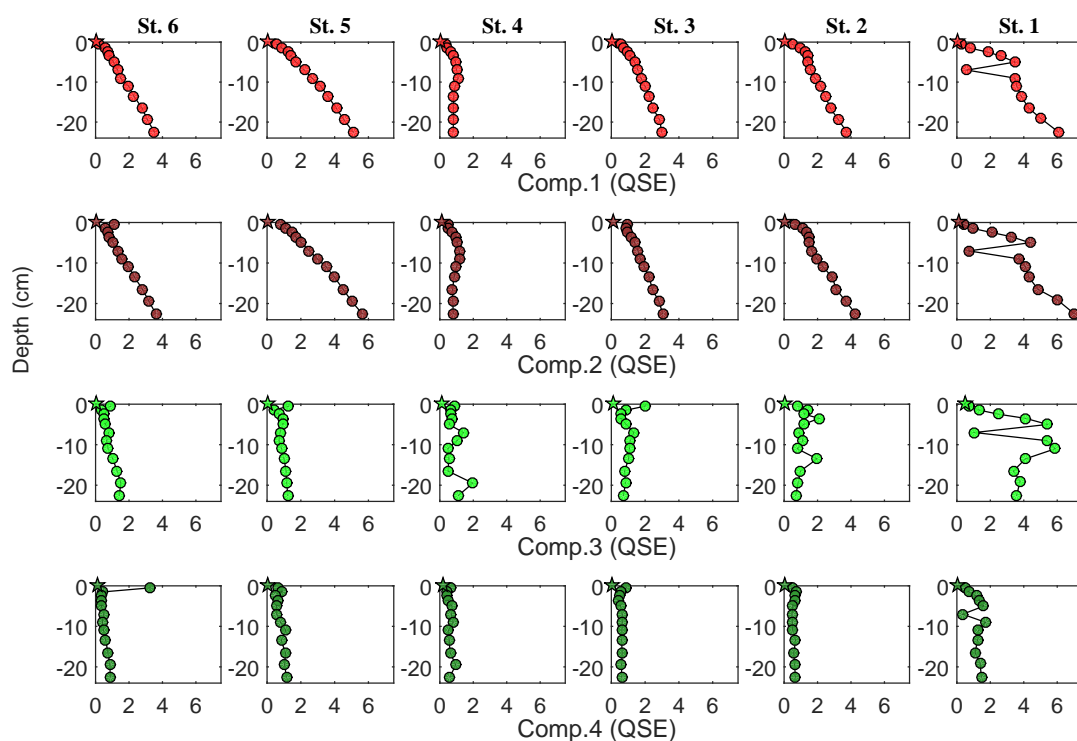


**Figure 7.** Pore water FDOM components distribution within the sediments: depth profiles. Humic-like Comp.1 and Comp.2 represented by light and dark red symbols, respectively. Amino acid-like Comp.3 and Comp.4 represented by light and dark green symbols, respectively. Circles represent concentration/value, measured in the pore water sample, pentagons represent the initial concentration/value of the bottom water.

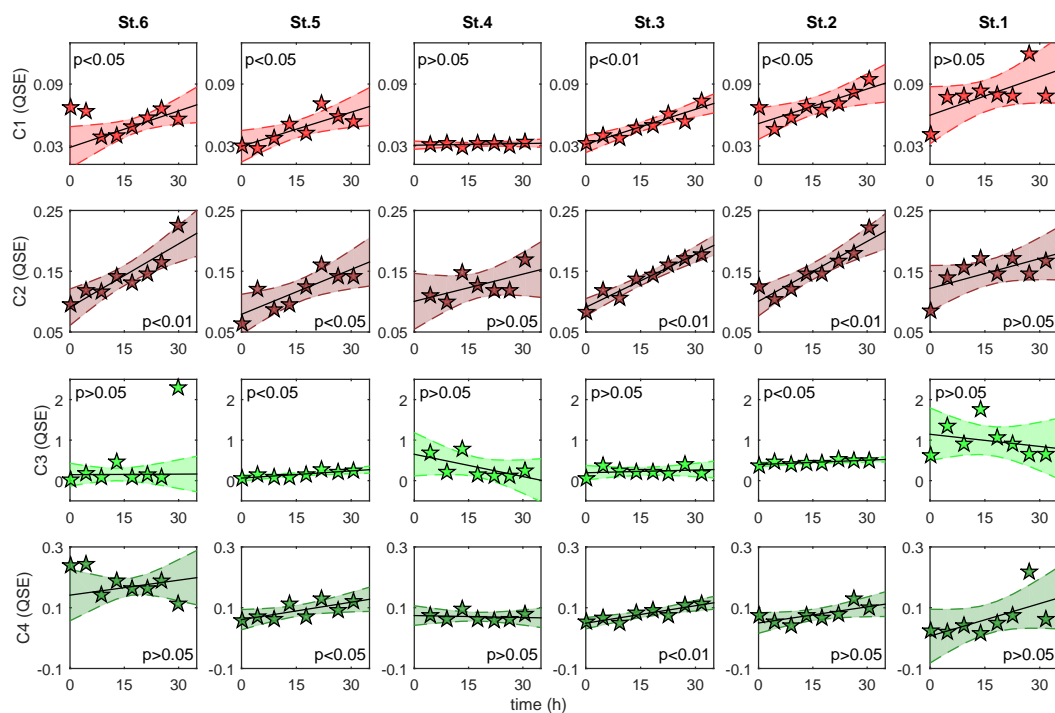


**Figure 8.** Distribution of FDOM components, measured in BIGO chambers over time. Polynomial fit (1st order) was used for linear regression analyses:  $t_0$  and data included in brackets were excluded from the analyses.

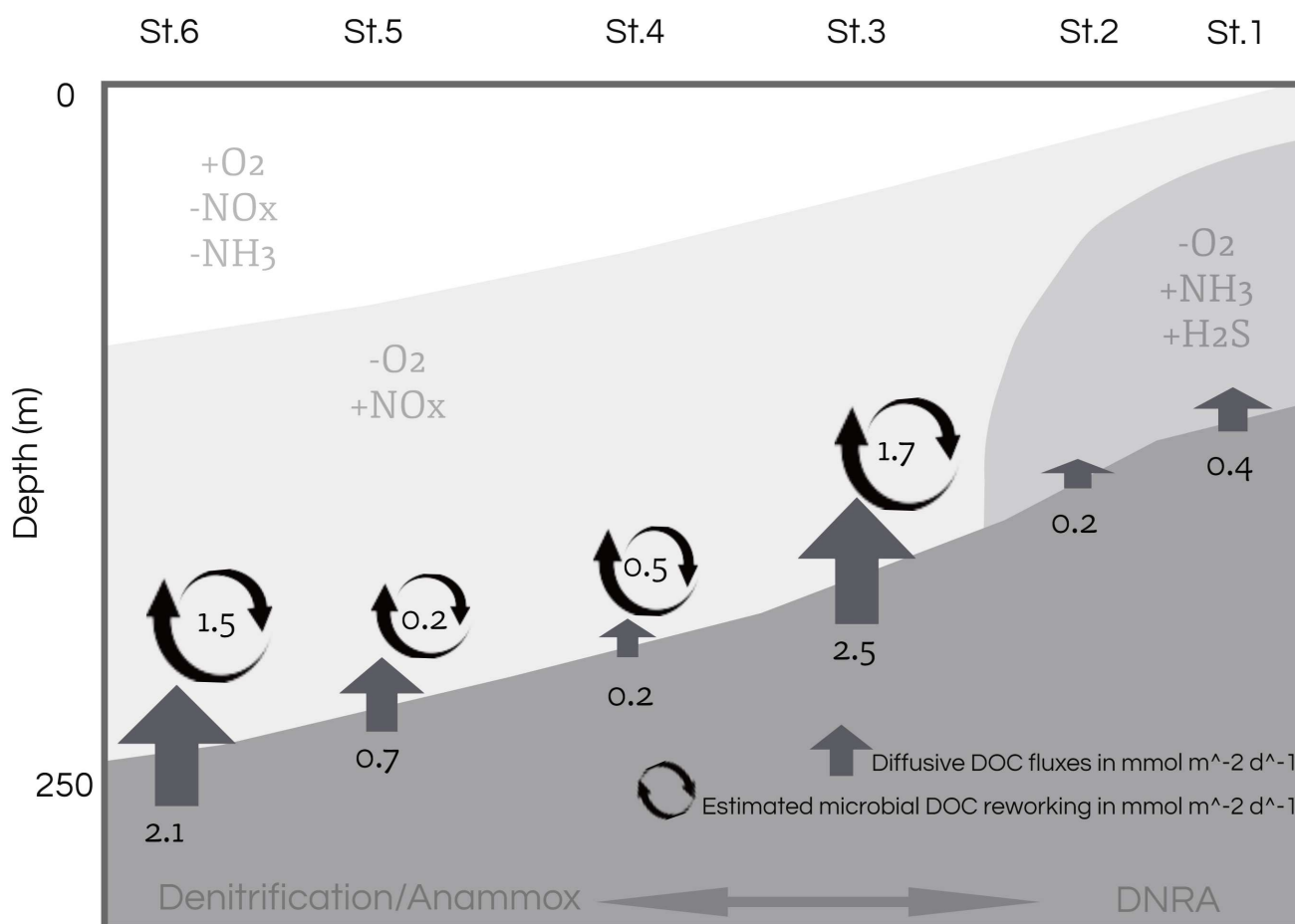


**Figure 9.** Conceptual view of DOM cycling near the sediment off Peru. Grey arrows represent the diffusive fluxes of DOC ( $J_{DOC}(Diff.)$ ) in  $\text{mmol m}^{-2} \text{d}^{-1}$ . Black arrows indicate microbial DOM reworking, calculated as a difference of  $J_{DOC}(Diff.)$  and net *in situ* flux ( $J_{DOC}(Net)$ ) at each station.



**Table 1.** Stations and instruments deployed during our study on the Peruvian margin.

Station	BIGO	MUC	Date (BIGO)	Date (MUC)	Latitude (°N)	Longitude (°E)	Depth (m)	Temp. (°C)	Porosity	O <sub>2</sub> (mol kg <sup>-1</sup> )	Dale et al. (2015)
St.1	533 BIGO II-IV	483 MUC 8	27 Apr	24 Apr	-77.180	-12.225	74	16.2	0.93	b.d.	Inner Shelf
St.2	642 BIGO II-II	577 MUC 11	09 May	01 May*	-77.212	-12.248	102	15.9	0.96	11	
St.3	488 BIGO II-III	426 MUC 6	24 Apr	19 Apr	-77.250	-12.280	128	15.2	0.95	b.d.	Outer Shelf
St.4	503 BIGO I-III	651 MUC 8	25 Apr	10 May	-77.297	-12.312	144	14.6	0.94	b.d.	
St.5	471 BIGO I-II	692 MUC 15	23 Apr	13 May	-77.362	-12.358	194	13.9	0.95	b.d.	
St.6	415 BIGO II-I	412 MUC 5	18 Apr	18 Apr	-77.403	-12.388	243	12.9	0.95	b.d.	Continental Slope

\* NH<sub>4</sub><sup>+</sup> concentrations were measured at 787MUC33 on 20<sup>th</sup> of May at -12.247°N and -77.212°E. Station depth was recorded from the ship winch. Bottom water temperature and O<sub>2</sub> are recorded by CTD. "b.d." stands for "below detection". Detection limit of O<sub>2</sub> is 5 μmol kg<sup>-1</sup> (Dale et al., 2015). Porosity is given for the upper 0.5 cm.